The Plant Cell, Vol. 32: 186–205, January 2020, www.plantcell.org © 2020 ASPB.

PHYTOCHROME INTERACTING FACTOR8 Inhibits Phytochrome A-Mediated Far-Red Light Responses in Arabidopsis

Jeonghwa Oh,[1] Eunae Park,[1] Kijong Song, Gabyong Bae, and Giltsu Choi[2]

Department of Biological Sciences, Korea Advanced Institute of Science and Technology, Daejeon 34141, Korea

ORCID IDs: 0000-0002-1887-7041 (J.O.); 0000-0002-1816-2732 (E.P.); 0000-0001-9038-8990 (K.S.); 0000-0001-8881-8349 (G.B.); 0000-0001-9962-8321 (G.C.).

PHYTOCHROME INTERACTING FACTORs (PIFs) are a group of basic helix-loop-helix (bHLH) transcription factors that repress plant light responses. PIF8 is one of the less-characterized Arabidopsis (*Arabidopsis thaliana*) PIFs, whose putative orthologs are conserved in other plant species. PIF8 possesses a bHLH motif and an active phytochrome B motif but not an active phytochrome A motif. Consistent with this motif composition, PIF8 binds to G-box elements and interacts with the Pfr form of phyB but only very weakly, if at all, with that of phyA. PIF8 differs, however, from other PIFs in its protein accumulation pattern and functional roles in different light conditions. First, PIF8 inhibits phyA-induced seed germination, suppression of hypocotyl elongation, and randomization of hypocotyl growth orientation in far-red light, but it does not inhibit phyB-induced red light responses. Second, PIF8 protein accumulates more in far-red light than in darkness or red light. This is distinct from the pattern observed with PIF3, which accumulates more in darkness. This PIF8 accumulation pattern requires degradation of PIF8 by CONSTITUTIVE PHOTOMORPHOGENIC1 (COP1) in darkness, inhibition of COP1 by phyA in far-red light, and promotion of PIF8 degradation by phyB in red light. Together, our results indicate that PIF8 is a genuine PIF that represses phyA-mediated light responses.

INTRODUCTION

Plants have evolved significant developmental plasticity to ensure their survival in the face of changing environmental conditions. Of the many environmental factors influencing plant development, light is one of the most critical (Franklin and Quail, 2010). In the dark, seedlings display skotomorphogenic phenotypes characterized by elongated hypocotyls with closed cotyledons and an exaggerated apical hook. These are developmental adjustments by which germinating seedlings can rapidly push through the soil without harming the shoot apical meristem. Once the seedlings emerge from the soil, skotomorphogenesis is suppressed, and the seedlings display photomorphogenic phenotypes characterized by short hypocotyls with open cotyledons and fully developed chloroplasts that are ready for photosynthesis. Plants have developed several classes of photoreceptors that detect and respond to light quality, quantity, duration, and direction (Galvão and Fankhauser, 2015; Li and Mathews, 2016). Phytochromes (phyA to phyE in Arabidopsis [*Arabidopsis thaliana*]) are chromophore-conjugated dimeric proteins responsible for detecting far-red and red light (Clack et al., 1994; Rockwell et al., 2006; Li et al., 2015). Far-red and red light induce reversible conformational changes in phytochromes such that they take either the biologically inactive Pr form or the biologically active Pfr form, respectively. Pfr phytochromes enter the nucleus and promote photomorphogenesis, partly by inhibiting basic helix-loop-helix (bHLH) transcription factors called PHYTOCHROME INTERACTING FACTORs (PIFs) and ubiquitin E3 ligase complexes called CONSTITUTIVE PHOTOMORPHOGENIC1/SUPPRESSOR OF PHYA-105 complexes (COP1/SPAs; Nagatani, 2004; Bae and Choi, 2008; Leivar and Quail, 2011; Klose et al., 2015; Xu et al., 2015; Hoecker, 2017). In addition to detecting external light conditions, phytochromes also seem to sense ambient temperature. Pfr phytochromes are gradually converted to their Pr forms by thermal reversion, a process that is accelerated by increasing ambient temperature (Jung et al., 2016; Legris et al., 2016).

PIFs are bHLH transcription factors that possess a phyA binding APA (active phytochrome A) motif or a phyB binding APB (active phytochrome B) motif (Khanna et al., 2004; Al-Sady et al., 2006). They bind to G-box (CACGTG) motifs either alone or together with other transcription factors, including group A bZIPs like ABA INSENSITIVE5 (Martínez-García et al., 2000; Huq and Quail, 2002; Huq et al., 2004; Oh et al., 2007, 2009; Leivar et al., 2008b; Hornitschek et al., 2009, 2012; Kidokoro et al., 2009; Li, 2012; Zhang et al., 2013; Li et al., 2014; Pfeiffer et al., 2014; Kim et al., 2016b). Upon binding to their target promoters, PIFs recruit transcriptional regulators like LEUNIG_HOMOLOG, HEMERA, TIMING OF CAB EXPRESSION1, and HISTONE DEACETYLASE15 to either positively or negatively regulate gene expression (Yamashino et al., 2003; Liu et al., 2013; Lee et al., 2015; Qiu et al., 2015; Soy et al., 2016; Zhu et al., 2016; Gu et al., 2017; Qiu et al., 2019). PIFs promote skotomorphogenic development in the dark through this regulation of target gene expression. PIFs are found in all land plants ranging from liverwort to angiosperms (Llorente et al., 2016; Rosado et al., 2016; Lee and Choi, 2017; Xu and

[1] These authors contributed equally to this work.
[2] Address correspondence to gchoi@kaist.edu.
The author responsible for distribution of materials integral to the findings presented in this article in accordance with the policy described in the Instructions for Authors (www.plantcell.org) is: Giltsu Choi (gchoi@kaist.edu).
www.plantcell.org/cgi/doi/10.1105/tpc.19.00515

IN A NUTSHELL

Background: When plants are in the dark, their stems get longer to search for light. When reaching the light, plant photoreceptors called phytochromes perceive light and signal the plant body to adapt to the light environment. Phytochrome A (phyA) and phyB are two major phytochromes perceiving far-red light and red light, respectively. Upon light perception, phyA and phyB promote light responses partly by inhibiting Phytochrome interacting factors (PIFs). In a model plant, *Arabidopsis thaliana*, eight different PIFs (PIF1 to PIF8) regulate light responses both redundantly and distinctively.

Question: Among the eight different PIFs, the role of PIF8 had not been fully understood. Thus, we decided to characterize the role of PIF8 in light signaling by focusing on its similarities and differences to other better-characterized PIFs.

Findings: We found that *Arabidopsis* seedlings overexpressing PIF8 had longer hypocotyls with smaller and closed cotyledons than wild-type seedlings (that had short hypocotyls with larger and fully-opened cotyledons) in far-red light but not in red light. This was in contrast to seedlings overexpressing PIF3, which had those phenotypes in red light but not in far-red light. Such a far-red light-specific role of PIF8 is largely dictated by the far-red light-specific accumulation of PIF8 protein shaped by the interplay among phyA, phyB, and CONSTITUTIVE PHOTOMORPHOGENIC 1 (COP1), coupled with the resistance to be sequestered by phyA in far-red light. Accumulated and unsequestered PIF8 binds to target gene promoters and regulates gene expression, repressing light responses in far-red light.

Next steps: PIF8 is a well-conserved PIF, implying it provides advantages to plants living in natural light environments. Thus, it would be interesting to determine if PIF orthologs from other plant species have similar roles and to identify natural light conditions where PIF8 plays a role.

Hiltbrunner, 2017; Gao et al., 2019). *Chara braunii*, which belongs to the Charophyta clade, possesses a protein containing a distantly related APA motif, suggesting that PIF-like proteins may have evolved even before the emergence of land plants (Possart et al., 2017). Multiple PIFs are present in most land plant species with the exception of *Marchantia polymorpha*, a liverwort with only one PIF (Inoue et al., 2016). Arabidopsis possesses at least eight PIFs (PIF1 to PIF8), which regulate light responses either redundantly or distinctively (Jeong and Choi, 2013; Pham et al., 2018c). Among them, PIF1 specifically inhibits seed germination, whereas most PIFs redundantly promote skotomorphogenic phenotypes partly through their ability to promote cell elongation (Oh et al., 2004; Leivar and Monte, 2014). The redundant roles of the PIFs are exemplified by the constitutively photomorphogenic phenotypes of the *pif quadruple* mutant (*pif1 pif3 pif4 pif5*) in the dark (Leivar et al., 2008a; Shin et al., 2009).

Phytochromes inhibit PIFs in part by promoting PIF protein degradation. Light-activated Pfr interacts with and phosphorylates PIFs by kinase activity either intrinsic to the phytochromes or, as is the case for PIF3, by PHOTOREGULATORY PROTEIN KINASEs (PPK1 to PPK4) that are associated with phyB (Al-Sady et al., 2006; Ni et al., 2013, 2017; Shin et al., 2016). The phosphorylated PIFs are then polyubiquitinated and subsequently degraded by 26S proteasomes (Bauer et al., 2004; Park et al., 2004; Shen et al., 2005, 2007, 2008; Oh et al., 2006; Nozue et al., 2007; Lorrain et al., 2008). A few E3 ubiquitin ligases have been identified that ubiquitinate PIFs for degradation. Among the E3 ligase components, COLD TEMPERATURE-GERMINATING10 and EIN3 BINDING F-BOX PROTEINs promote light-induced degradation of PIF1 and PIF3, respectively (Dong et al., 2017; Majee et al., 2018). BLADE-ON-PETIOLEs ubiquitinate PIF4 for degradation in red light (Zhang et al., 2017), while LIGHT-RESPONSIVE BRIC-A-BRACK/TRAMTRACK/BROADs bind to the Pfr form of phyB and PIF3 and ubiquitinate them, ensuring their destruction in the presence of red light (Ni et al., 2014). PIFs are also phosphorylated independently of light by protein kinases such as CASEIN KINASE II and BRASSINOSTEROID-INSENSITIVE2 (BIN2; Bu et al., 2011; Ling et al., 2017). In addition to PIF protein degradation, phyB inhibits PIFs by sequestering them from their target gene promoters (Park et al., 2012, 2018).

COP1 is a RING-type E3 ubiquitin ligase that suppresses photomorphogenesis in association with SPA proteins (Huang et al., 2014; Hoecker, 2017). COP1/SPAs suppress photomorphogenesis by directly ubiquitinating and degrading photomorphogenesis-promoting factors including ELONGATED HYPOCOTYL5 (HY5) and LONG HYPOCOTYL IN FAR-RED1 (HFR1) in the dark (Osterlund et al., 2000; Hoecker and Quail, 2001; Duek et al., 2004; Jang et al., 2005; Yang et al., 2005). COP1 also regulates PIF protein stability: it promotes the degradation of PHYTOCHROME INTERACTING FACTOR3-LIKE1 (PIL1/PIF2; Luo et al., 2014) but increases the stability of PIF1, PIF3, PIF4, and PIF5 in the dark (Bauer et al., 2004; Pham et al., 2018a, 2018b). During the dark-to-light transition, COP1 also ubiquitinates PIF1 and PIF5, promoting their degradation (Shen et al., 2008; Zhu et al., 2015; Pham et al., 2018b). Phytochromes inhibit COP1/SPAs either by excluding COP1 from the nucleus (von Arnim and Deng, 1994; Osterlund and Deng, 1998; Pacín et al., 2013, 2014), by disrupting COP1/SPA complexes (Lu et al., 2015; Sheerin et al., 2015), or by degrading SPA proteins (Balcerowicz et al., 2011; Chen et al., 2015). Such inhibition of COP1/SPAs by phytochromes results in the accumulation of several different factors, including HY5, that promote photomorphogenic development in the light.

PIF8 is one of the more poorly characterized PIFs in Arabidopsis (Leivar and Quail, 2011). Given the importance of the other PIFs in light signaling, however, PIF8 too likely plays an important role in

light signaling. Here, we report that PIF8 binds to the Pfr form of phyB but only very weakly, if at all, to that of phyA. We found that PIF8, unlike other PIFs, suppresses phyA-mediated far-red light responses, including seed germination and seedling photomorphogenesis, without affecting phyB-mediated responses to red light. PIF8 protein levels are higher under far-red light illumination than in the dark or under red light. This is in contrast to the levels of the other PIFs, which are higher in the dark than under red or far-red light. This increased accumulation of PIF8 under far-red light is caused by the combination of phyA-mediated inhibition of COP1 under far-red light, COP1-mediated degradation of PIF8 in the dark, and the promotion of PIF8 degradation by phyB in red light. Together, these findings indicate that PIF8 is a genuine PIF that mitigates excessive photomorphogenic seedling development in prolonged far-red light.

RESULTS

PIF8 Binds to Pfr of phyB but Only Very Weakly, if at All, to That of phyA

PIF8, also denoted as UNFERTILIZED EMBRYO SAC10, is one of the less-characterized PIFs possessing a bHLH domain and an APB motif but not a core APA motif (Figure 1A). PIF8 is more similar to PIF7 than to the other Arabidopsis PIFs, and its orthologs are found in other plant species including tomato (*Solanum lycopersicum*) and rice (*Oryza sativa*; Figure 1B; Supplemental Figure 1; Supplemental Files 1 and 2). Compiled transcriptome data indicate that *PIF8* mRNA is expressed at higher levels in leaves than in seeds, and its expression pattern resembles that of *PIF4*, *PIF5*, and *PIF7* rather than *PIF1* and *PIF3* (Figure 1C; Supplemental Figure 2). Our experiments further indicate that *PIF4*, *PIF5*, *PIF7*, and *PIF8* mRNA levels are increased by both red and far-red light, whereas *PIF1* and *PIF3* mRNA levels are not (Figure 1D). Light-induced expression of *PIF8* mRNA is abolished in the *phyA-211* (*phyA*) mutant under far-red light and in the *phyB-9* (*phyB*) mutant under red light (Figure 1E). These results suggest that PIF8, which is expressed in a pattern similar to PIF4, PIF5, and PIF7 in Arabidopsis, could be a genuine member of the conserved PIF family in angiosperms.

PIF8 possesses a conserved APB motif but lacks a core APA motif (Figure 1A). This suggests that it is capable of binding phyB but not phyA. We therefore examined whether PIF8 protein can directly interact with phyA and phyB in vitro and in vivo. We performed in vitro binding assays using recombinant glutathione S-transferase (GST)-tagged PIF8 and MYC-tagged phyA or phyB proteins. We found that PIF8 preferentially binds to the Pfr form of phyB, but it does not bind to phyA regardless of its form (Figure 2A). Unlike PIF8, PIF3 shows preferential binding to the Pfr form of both phyA and phyB in the same binding assays. Although we used the same amount of PIF8 and PIF3 protein, we found that PIF8 was capable of pulling down less phyB than PIF3, suggesting that PIF8's binding affinity for phyB is weaker than that of PIF3. We also performed semi-in vivo binding assays using recombinant GST-tagged PIF8 and cell extracts from transgenic lines expressing FLAG-tagged phyA or phyB. As with the in vitro binding assays, PIF8 preferentially pulls down the Pfr form of phyB but only very weakly, if at all, that of phyA from cell extracts, while PIF3 pulls down the Pfr form of both phyA and phyB (Figure 2B). Also similar to the in vitro binding assays, PIF8's affinity for phyB is weaker than that of PIF3. In in vivo binding assays using transgenic lines expressing MYC-tagged PIF8 or PIF3 (*PIF8-OX* and *PIF3-OX*), we found further evidence that PIF8 preferentially coimmunoprecipitates the Pfr form of phyB but only very weakly, if at all, that of phyA, while PIF3 coimmunoprecipitates the Pfr form of both phyA and phyB (Figure 2C).

PIF8 Inhibits a Subset of phyA-Induced Light Responses in Prolonged Far-Red Light

To investigate the biological roles of PIF8, we generated transgenic lines expressing MYC-tagged PIF8 under the control of the 35S promoter (*PIF8-OX*) and isolated two *pif8* mutants (*pif8-1* and *pif8-2*). The *pif8-1* mutant has a T-DNA insertion in the fourth intron, while *pif8-2* is a clustered regularly interspaced short palindromic repeats (CRISPR)-CAS-generated mutant with a single nucleotide insertion in the first exon that leads to the formation of a premature stop codon (Figure 3A).

In far-red light, *PIF8-OX* produces hypocotyls twice as long as those of the wild type (Columbia-0 [Col-0]), but in the dark and in red light, its hypocotyls are similar to those of the wild type (Figures 3B and 3C). When compared with wild-type seedlings in far-red light, *PIF8-OX*, like the *phyA* mutant, produces more closed cotyledons (Figure 3B) and expresses higher levels of the marker genes *PIL1* and *PIL2* (Supplemental Figure 3). The two *pif8* mutants, however, produce hypocotyls similar in length to those of the wild type regardless of the light conditions. The wild-type-like hypocotyls of the *pif8* mutants may be due to PIF8's redundancy with other PIFs. Since *PIF8* is expressed in a similar pattern to *PIF4*, *PIF5*, and *PIF7* (Figure 1C), we generated and examined the phenotypes of mutants lacking multiple PIFs. Consistent with the redundancy hypothesis, the *pif4 pif5 pif8* (*pif458*) triple mutant produces small but significantly shorter hypocotyls than the *pif4 pif5* (*pif45*) double mutant in far-red light (Figure 3C). The *pif7 pif8* (*pif78*) double mutant also produces small but significantly shorter hypocotyls than the *pif7* single mutant in far-red light. We further examined the role of PIF8 in phyA and phyB signaling by generating *pif8 phyA* and *pif8 phyB* double mutants. The *pif8 phyA* double mutant produces hypocotyls identical in length to those of the *phyA* single mutant under far-red light, whereas the *pif8 phyB* double mutant produces hypocotyls shorter than those of the *phyB* mutant but similar to those of the *pif8* mutant under far-red light (Supplemental Figure 4). Together, these results indicate that PIF8 inhibits phyA-induced seedling photomorphogenesis redundantly with PIF4, PIF5, and PIF7 in far-red light.

We next examined whether PIF8 also regulates any other phyA-mediated far-red light responses such as seed germination or hypocotyl negative gravitropism. More than 80% of wild-type seeds germinate by 12 h of far-red light irradiation in phyA-dependent germination assays, while *PIF8-OX* seeds, like *phyA* mutant seeds, do not germinate even by 24 h of far-red light irradiation (Figure 4A). These low germination frequencies for *PIF8-OX* seeds are not due to death or dormancy, because more than 80% of *PIF8-OX* seeds germinate in phyB_ON or white light conditions (Figure 4B). These results indicate that PIF8 inhibits

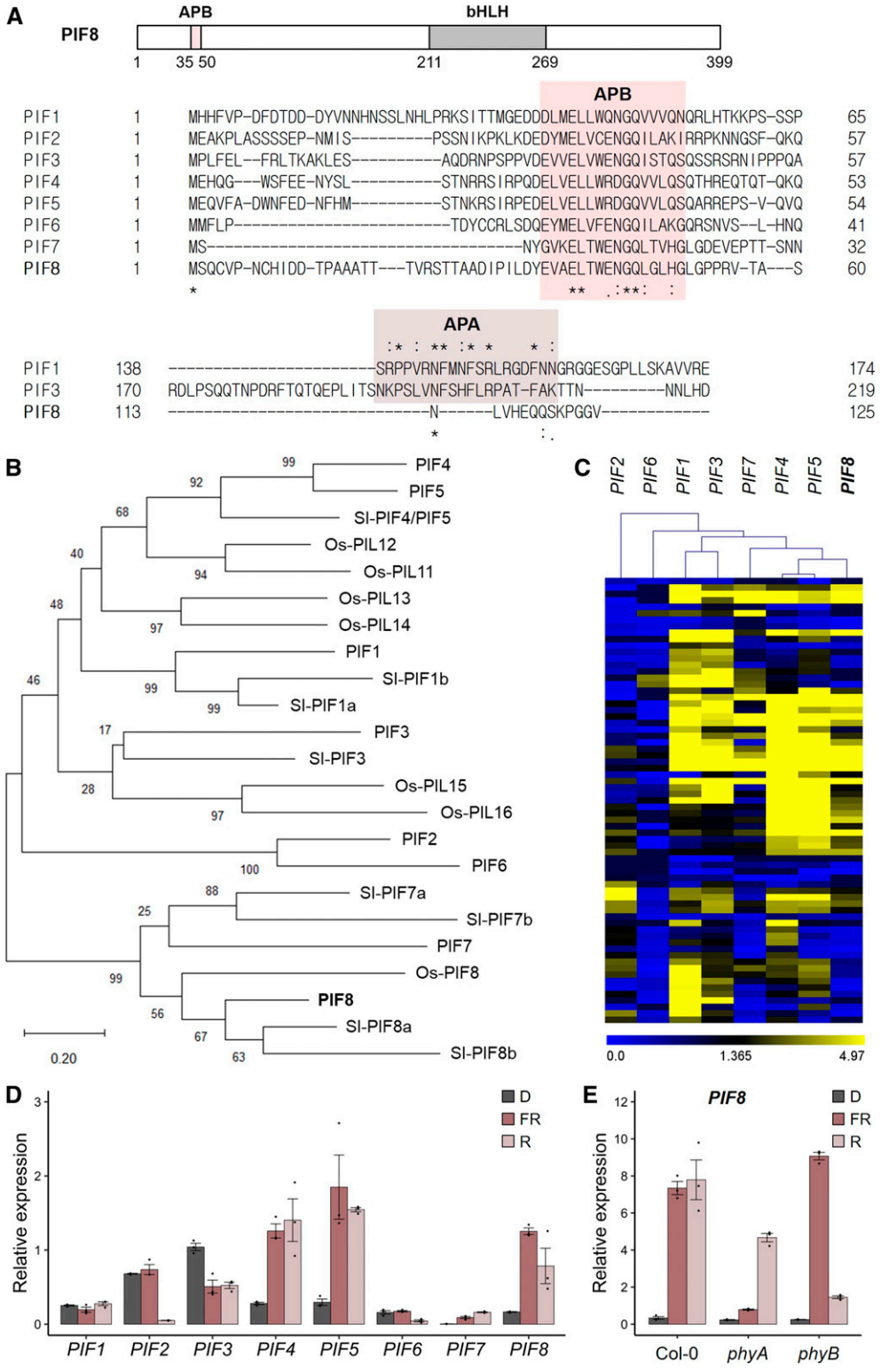

Figure 1. PIF8 Is an APB-Containing bHLH Transcription Factor.

(A) A diagram showing the APB and bHLH motifs of PIF8 protein. The numbers are amino acid residue numbers. The bottom panel shows the amino acid sequence alignments of PIF8 with the other PIFs at their APA and APB motifs. Only PIF1 and PIF3, which possess the conserved APA motif, were used for the

phyA-induced seed germination. PIF8 also regulates hypocotyl negative gravitropism in far-red light (Figure 4C). Wild-type seedlings grow upward against gravity in the dark, displaying hypocotyl negative gravitropism, whereas seedlings lie down both in red and far-red light, displaying hypocotyl agravitropism. Unlike wild-type seedlings, *phyA* and *phyB* mutant seedlings grow upward not only in the dark but also in far-red and red light, respectively, supporting a role for phyA and phyB in inhibiting hypocotyl negative gravitropism in response to far-red and red light, respectively. *PIF8-OX* seedlings grow upward against gravity in far-red light but lie down in red light. These results indicate that PIF8 suppresses phyA-mediated inhibition of hypocotyl negative gravitropism in far-red light. Phytochromes are capable of disrupting hypocotyl negative gravitropism, in part by inhibiting the PIFs that maintain starch-filled endodermal amyloplasts (Kim et al., 2011). Consistent with this, *PIF8-OX* seedlings, like *phyA* mutants, retain their starch-filled endodermal amyloplasts in far-red light, whereas wild-type seedlings do not (Figure 4D). These results indicate that PIF8 promotes hypocotyl negative gravitropism by inhibiting the depletion of starch-filled amyloplasts in far-red light.

We next measured shade-induced hypocotyl elongation in *PIF8-OX*. Shade inactivates phyB, releasing PIFs and promoting shade responses. At the same time, however, shade also activates phyA, inhibiting shade responses (Franklin, 2008; Roig-Villanova and Martínez-García, 2016). The magnitude of a seedling's shade response is thus determined by integration of these opposing effects of phyA and phyB. We measured the hypocotyls of seedlings grown under either high or low red:far-red light. We found that the hypocotyls of wild-type seedlings grow 2.5 times longer when grown under low red:far-red light (shade) than under high red:far-red light (normal; Supplemental Figure 5). Consistent with the opposing roles for phyA and phyB in driving shade responses, the hypocotyls of *phyA* mutant seedlings are longer than those of wild-type seedlings grown in the shade, whereas the hypocotyls of *phyB* mutant seedlings are longer than those of wild-type seedlings even in high red:far-red light. Shade-induced hypocotyl elongation is promoted in part by PIF4, PIF5, and PIF7 (Lorrain et al., 2008; Li et al., 2012). Consistent with this, the hypocotyls of *pif45* and *pif7* mutant seedlings grown in the shade are shorter than those of the wild type. Unlike those of *pif45* and *pif7* mutants, however, the hypocotyls of *pif8* mutant seedlings grown in the shade are similar to those of the wild type. The hypocotyls of *pif458* triple and *pif78* double mutant seedlings are also similar to those of *pif45* and *pif7* mutants grown in the shade, respectively. Even the hypocotyls of *PIF8-OX* seedlings are similar to those of wild-type seedlings grown in the shade. These results indicate that, although phyA plays an active role in shade responses, PIF8 does not promote hypocotyl elongation in the shade.

PIF8 Is Stabilized by phyA but Destabilized by phyB

We next wondered how PIF8, expressed by the constitutive 35S promoter, promotes hypocotyl elongation only in far-red but not red light. Since phytochromes inhibit PIFs in part by promoting PIF protein degradation, we measured PIF8 protein levels under different light conditions using transgenic plants expressing MYC-tagged PIF8 or PIF3 under the control of the 35S promoter (*PIF8-OX* and *PIF3-OX*). Interestingly, we found more accumulation of PIF8 protein in far-red light than in either the dark or red light (Figure 5A). PIF3 protein, by contrast, accumulates more in the dark than under red light. To determine whether this unusual PIF8 protein accumulation pattern is due to PIF8's interactions with phytochromes, we generated *PIF8-OX* lines in the *phyA*, *phyB*, and *phyA phyB* (*phyAB*) mutant backgrounds by crossing *PIF8-OX* to each phytochrome mutant. We did not see any significant difference in the level of PIF8 protein produced in *phyA* mutant background seedlings (*PIF8-OX phyA*) grown under far-red light rather than in the dark, nor did we see any difference in PIF8 levels in *phyB* mutant background seedlings (*PIF8-OX phyB*) grown under red light rather than in the dark (Figure 5B). In the *phyAB* double mutant background (*PIF8-OX phyAB*), we found similar levels of PIF8 protein under all light conditions. Together, these results indicate that PIF8 protein is stabilized by phyA in far-red light and destabilized by phyB in red light. Curiously, we noticed that *phyB* mutants accumulate more PIF8 than the wild type under far-red light. As previously reported, this may be due to the inhibition of phyA signaling by phyB in far-red light (Wagner et al., 1996; Casal et al., 2000; Zheng et al., 2013). The hypocotyl lengths of *phyB* mutant seedlings, however, were identical to those of the wild type under far-red light in our experimental conditions. This

Figure 1. (continued).

APA motif alignment. The conserved APA and APB motifs are shaded. For the APA motif alignment, the symbols above the alignment indicate the level of conservation between PIF1 and PIF3: *, conserved sequences; :, conservative mutations; ., semiconservative mutations.

(B) The phylogenetic clustering of PIF8 with PIF7. The amino acid sequences of Arabidopsis, tomato, and rice PIFs and PILs were aligned, and a phylogenetic tree was drawn using the maximum-likelihood method with 500 bootstrap repeats. The numbers at each node represent the statistical probability (%) of each node in the bootstrap tests. Branch lengths represent the number of substitutions per site. Prefixes indicate species: Sl for tomato and Os for rice. Genes and proteins from Arabidopsis are noted without a prefix.

(C) The expression pattern clustering of *PIF8* with *PIF4*, *PIF5*, and *PIF7*. Expression levels of each *PIF* gene in various tissues and developmental stages were retrieved from the Klepikova Arabidopsis Atlas eFP browser (Klepikova et al., 2016), and their similarity was visualized by hierarchical clustering. See Supplemental Figure 2 for more detailed information.

(D) Light-inducible expression of *PIF8* as well as *PIF4*, *PIF5*, and *PIF7*. Four-day-old wild-type seedlings grown in various light conditions were used for the expression analysis of Arabidopsis PIFs. Expression analysis was performed by quantitative real-time PCR. D, dark; FR, far-red light (2.5 μmol m^{-2} s^{-1}); R, red light (15 μmol m^{-2} s^{-1}). Individual data points are indicated with dots. Error bars indicate SE ($n = 3$ biological replicates).

(E) phyA- and phyB-mediated light-inducible expression of *PIF8*. Seedlings were grown for 4 d in the dark (D), far-red light (FR; 2.5 μmol m^{-2} s^{-1}), or red light (R; 15 μmol m^{-2} s^{-1}) before being used for the expression analysis. Expression analysis was performed by quantitative real-time PCR. *phyA*, *phyA-211* mutant; *phyB*, *phyB-9* mutant. Individual data points are indicated with dots. Error bars indicate SE ($n = 3$ biological replicates).

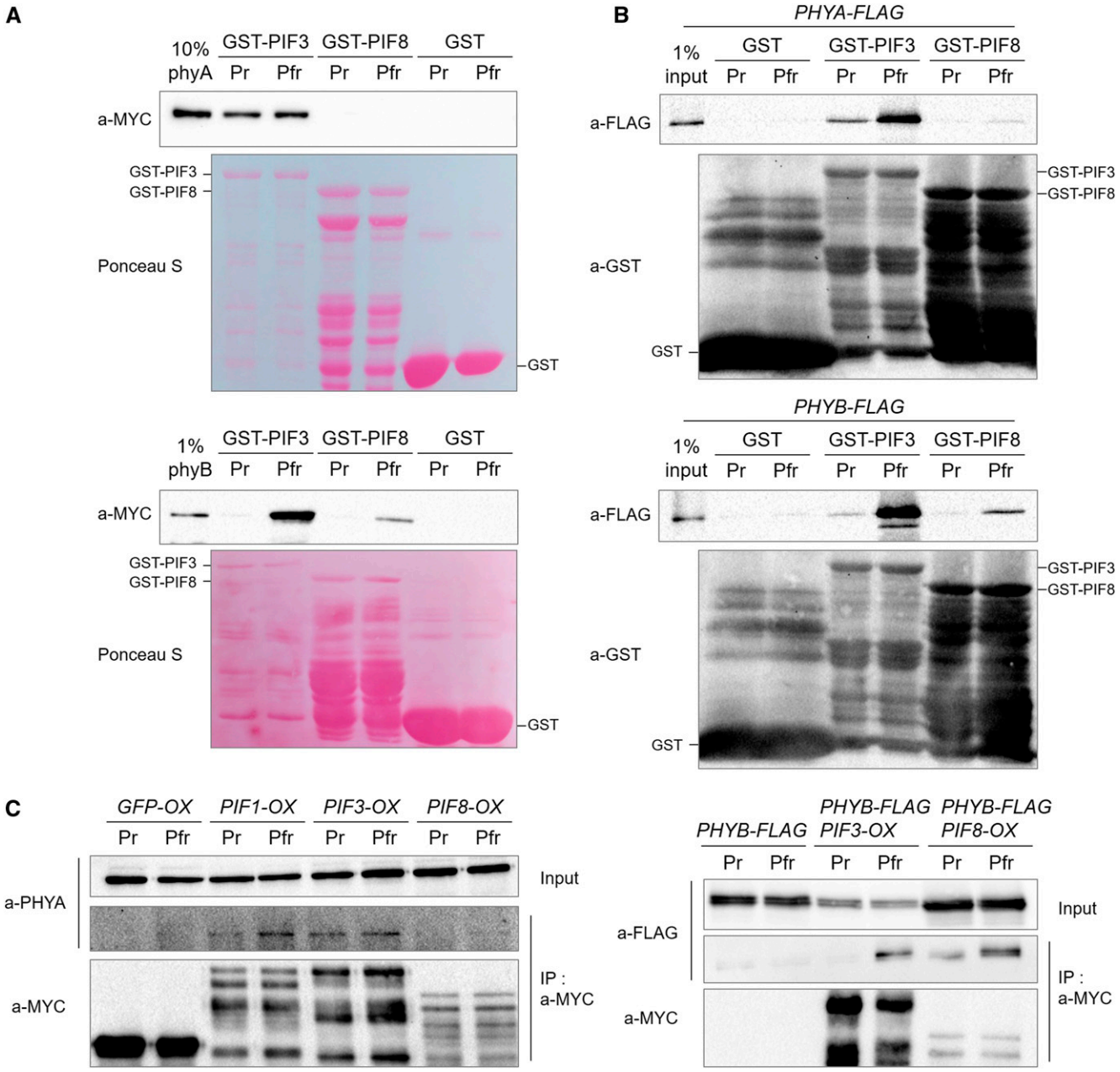

Figure 2. PIF8 Preferentially Binds to the Pfr Form of phyB but Not to That of phyA.

(A) In vitro binding assays showing preferential binding of PIF8 to the Pfr form of phyB but not phyA. Recombinant GST-PIF8 or GST-PIF3 was mixed with recombinant MYC-tagged phytochromes preirradiated with 5 min of far-red light (2.5 μmol m^{-2} s^{-1}) or red light (15 μmol m^{-2} s^{-1}) to generate the Pr or Pfr form, respectively. GST-tagged PIF proteins were pulled down with Glutathione Sepharose resin. Coprecipitated phytochromes were detected with a MYC-specific antibody (a-MYC). Ponceau S staining shows the amount of each GST-tagged PIF protein.

(B) Semi-in vivo binding assays showing preferential binding of PIF8 to the Pfr form of phyB but not phyA. Recombinant GST-PIF8 or GST-PIF3 was mixed with cell extracts of transgenic plants and irradiated for 5 min with far-red light (2.5 μmol m^{-2} s^{-1}) or red light (15 μmol m^{-2} s^{-1}). GST-tagged PIF proteins were pulled down with Glutathione Sepharose resin. Coprecipitated phytochromes were detected with a FLAG-specific antibody (a-FLAG). Four-day-old etiolated transgenic seedlings expressing either FLAG-tagged phyA (*PHYA-FLAG*) or phyB (*PHYB-FLAG*) were used to obtain cell extracts from transgenic plants.

(C) In vivo binding assays showing preferential binding of PIF8 to the Pfr form of phyB but not phyA. Four-day-old etiolated transgenic seedlings expressing MYC-tagged PIFs were irradiated for 30 min with far-red light (2.5 μmol m^{-2} s^{-1}) or red light (15 μmol m^{-2} s^{-1}). MYC-tagged PIF proteins were immunoprecipitated from cell extracts with a MYC-specific antibody (a-MYC). Coimmunoprecipitated phyA was detected with a phyA-specific antibody (a-PHYA), and phyB-FLAG was detected with a FLAG-specific antibody (a-FLAG).

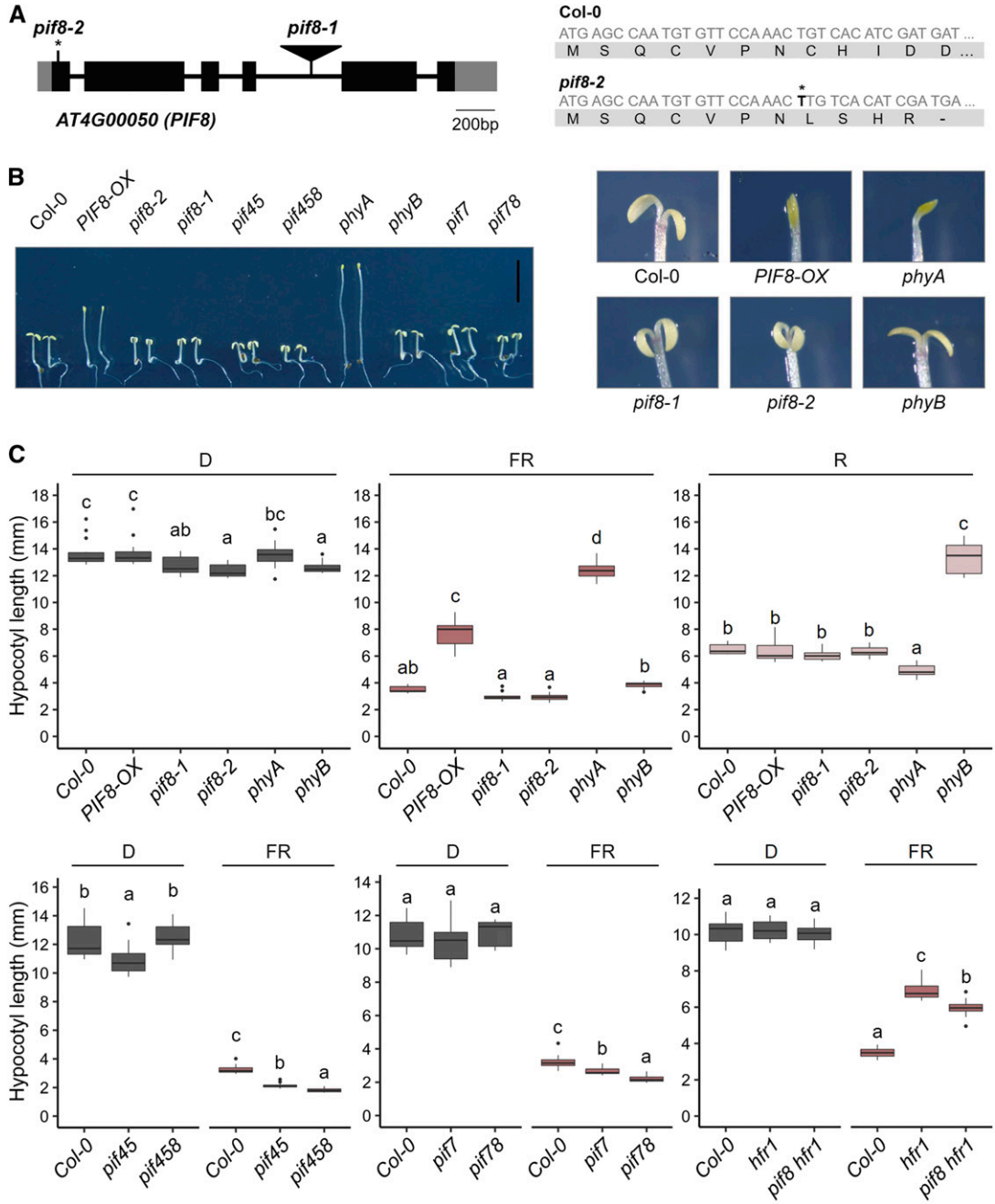

Figure 3. PIF8 Inhibits phyA-Induced Seedling Photomorphogenesis in Prolonged Far-Red Light.

(A) The genomic structure of the *PIF8* locus showing *pif8* mutation sites. Gray boxes, untranslated regions; black boxes, exons; black lines, introns; inverted triangle, *pif8-1* T-DNA insertion site; *, *pif8-2* thymidine insertion site. The right panel indicates the DNA and amino acid sequences of *pif8-2* showing the premature stop codon induced by a single thymidine insertion.

(B) Elongated hypocotyls and closed cotyledons of 4-d-old *PIF8-OX* seedlings grown in far-red light (1 μmol m^{-2} s^{-1}). The photograph on the left shows 4-d-old seedlings grown in far-red light, and the photographs on the right show cotyledon opening of 4-d-old seedlings grown in far-red light. Col-0, wild type; *PIF8-OX*, *PIF8*-overexpressing line; *pif8-1*, T-DNA insertion *pif8* mutant; *pif8-2*, CRISPR-CAS-generated *pif8* mutant; *phyA*, *phyA-211*; *phyB*, *phyB-9*; *pif45*, *pif4 pif5*; *pif458*, *pif4 pif5 pif8*; *pif78*, *pif7 pif8*. Bar = 5 mm.

(C) Box plots showing hypocotyl lengths of 4-d-old seedlings grown in the dark (D), far-red light (FR; 1 μmol m^{-2} s^{-1}), or red light (R; 15 μmol m^{-2} s^{-1}). The borders of the boxes indicate the 25th and 75th percentiles. The horizontal line indicates the median, and the whiskers span 1.5 times the interquartile range. Outliers are depicted as black dots. The letters above each box indicate statistical significance as determined by an ANOVA with Tukey's HSD posthoc test for multiple comparisons. Levels that are not significantly different are marked with the same letter (n = 15 seedlings).

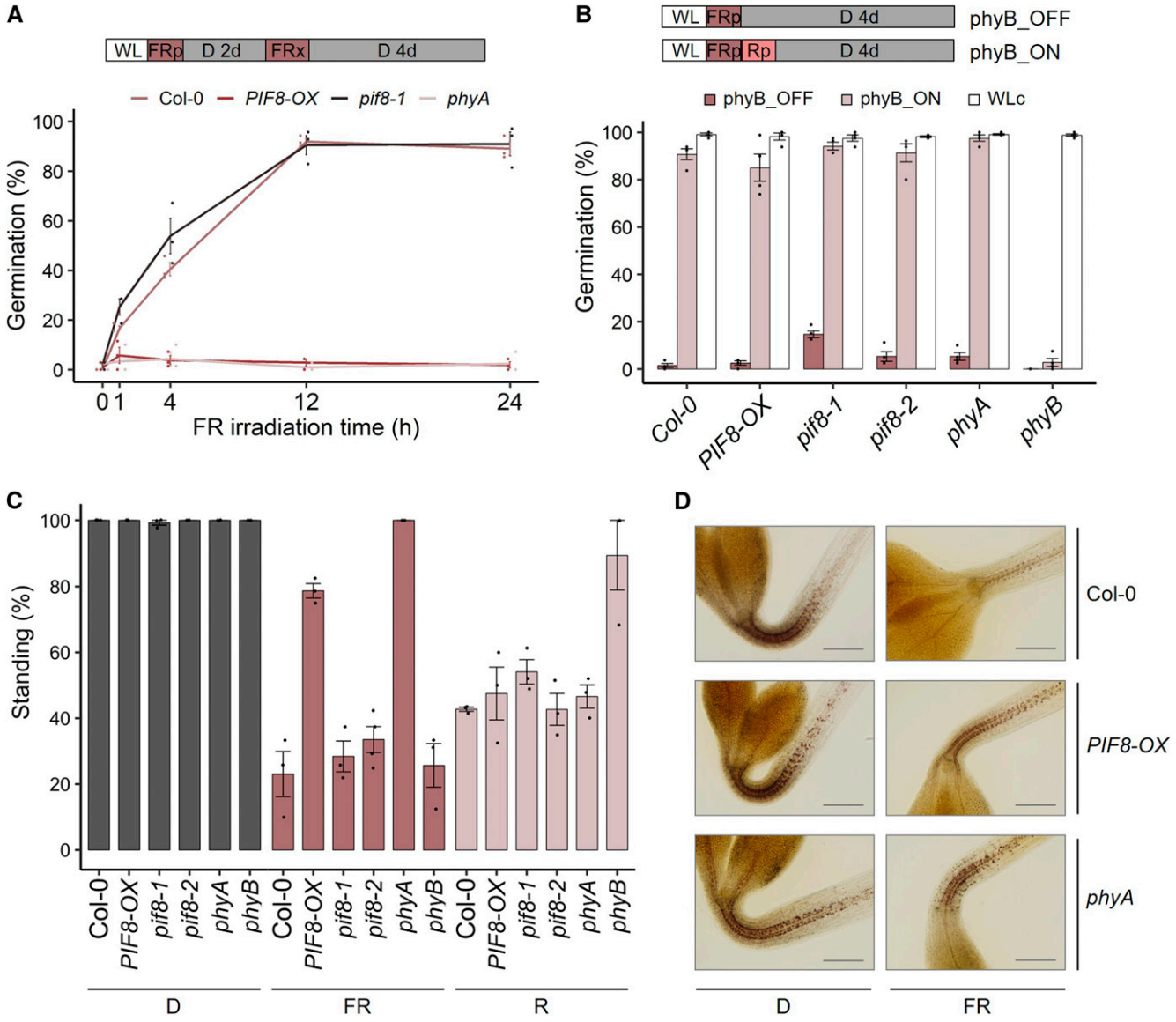

Figure 4. PIF8 Inhibits a Subset of phyA-Mediated Far-Red Light Responses.

(A) Inhibition of phyA-dependent germination by PIF8. The top diagram indicates a light irradiation scheme for phyA-dependent germination assays. The bottom graph indicates the germination frequencies for each genotype. WL, 1 h of white light (50 μmol m^{-2} s^{-1}) for seed sterilization and plating; FRp, far-red light pulse (2.5 μmol m^{-2} s^{-1}, 5 min); D 2d, 2 d at 22°C in the dark; FRx, *x* hours of far-red light (2.5 μmol m^{-2} s^{-1}); D 4d, 4 d at 22°C in the dark. Individual data points are indicated with dots. Error bars indicate SE ($n = 3$ biological replicates using different seedling samples).

(B) No inhibition of phyB-dependent germination by PIF8. Top diagrams indicate light irradiation schemes for the phyB_OFF and phyB_ON germination conditions. The bottom graph indicates the germination frequencies for each genotype. Rp, red light pulse (15 μmol m^{-2} s^{-1}, 5 min); WLc, 4 d in white light. Other notations are identical to those in **(A)**. Individual data points are indicated with dots. Error bars indicate SE ($n = 4$ biological replicates using different seedling samples).

(C) Promotion of hypocotyl negative gravitropism by PIF8 in far-red light. Seedlings were grown for 4 d in the vertical position under different light conditions, and then standing seedlings were counted. D, dark; FR, far-red light (1 μmol m^{-2} s^{-1}); R, red light (15 μmol m^{-2} s^{-1}). Individual data points are indicated with dots. Error bars indicate SE ($n = 3$ biological replicates using different seedling samples).

(D) Maintenance of starch-filled endodermal amyloplasts by PIF8 in far-red light. Seedlings were grown in the dark for 2 d and either kept in the dark (D) or transferred to far-red light (FR; 2.5 μmol m^{-2} s^{-1}) for 12 h. Amyloplasts are visualized by Lugol's iodine staining. Bars = 250 μm.

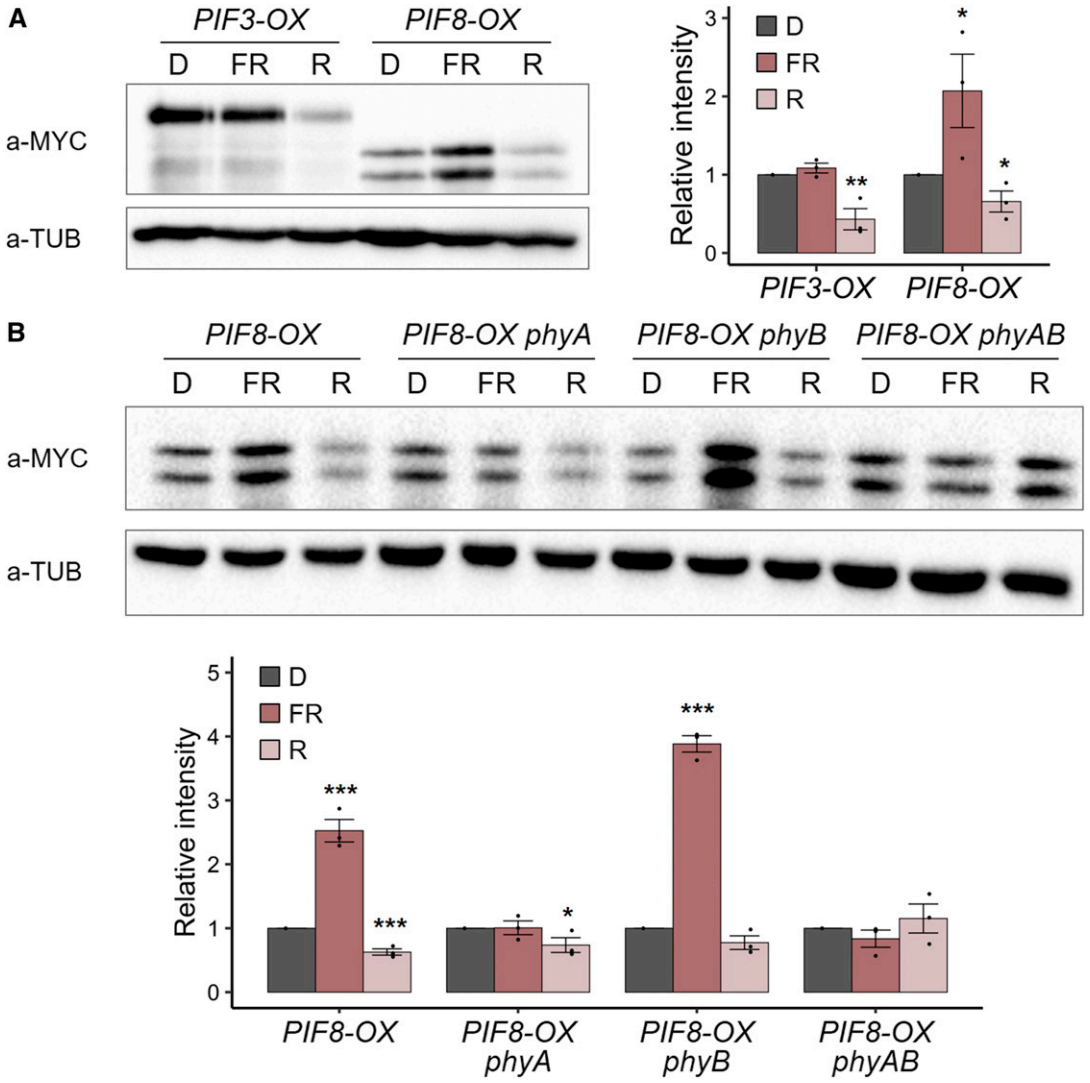

Figure 5. PIF8 Protein Accumulates in Far-Red Light but Not in the Dark.

(A) Selective accumulation of PIF8 protein in far-red light rather than in the dark or in red light. Transgenic seedlings expressing either MYC-tagged PIF8 (*PIF8-OX*) or MYC-tagged PIF3 (*PIF3-OX*) were grown in different light conditions for 4 d, and MYC-tagged PIF protein levels were measured by immunoblot. D, dark; FR, far-red light (2.5 μmol m^{-2} s^{-1}); R, red light (15 μmol m^{-2} s^{-1}). Relative intensities were determined by comparing the PIF protein band intensity with the tubulin band intensity. Intensities in the dark were set to 1 for each genotype. Individual data points are indicated with dots. Asterisks indicate significant differences from the dark values (*, $P < 0.05$; **, $P < 0.01$; and ***, $P < 0.001$; Student's *t* test). Error bars indicate SE ($n = 3$ biological replicates). a-MYC, anti-MYC antibody; a-TUB, anti-tubulin antibody.

(B) Stabilization of PIF8 protein by phyA in far-red light and destabilization of PIF8 protein by phyB in red light. The top panel shows immunoblots of PIF8 protein, and the bottom panel shows the quantification of the immunoblots. *phyA*, *phyA-211* mutant; *phyB*, *phyB-9* mutant; *phyAB*, *phyA-211 phyB-9* double mutant. Other notations are identical to those in **(A)**.

suggests that inhibition of phyA signaling by phyB under far-red light is relatively weak (Figure 3C; Supplemental Figure 4).

COP1 Ubiquitinates and Degrades PIF8 Protein in the Dark

Since phyA does not bind to PIF8, it is unclear how phyA stabilizes PIF8 protein in far-red light. One possibility is that PIF8 protein is actively degraded by a ubiquitin E3 ligase such as COP1/SPAs, and phyA inhibits this E3 ligase selectively in far-red light. To test this hypothesis, we treated seedlings with the 26S proteasome inhibitor MG132 and measured PIF8 protein levels. We found that MG132 treatment dramatically increases PIF8 protein levels in the dark but not in far-red light, supporting the hypothesis that PIF8 protein is actively degraded by the 26S proteasome in the dark (Figure 6A).

Many photomorphogenic factors, including HY5, HFR1, PHYTOCHROME RAPIDLY REGULATED1 (PAR1) and PAR2, are degraded by COP1 in the dark (Osterlund et al., 2000; Duek et al.,

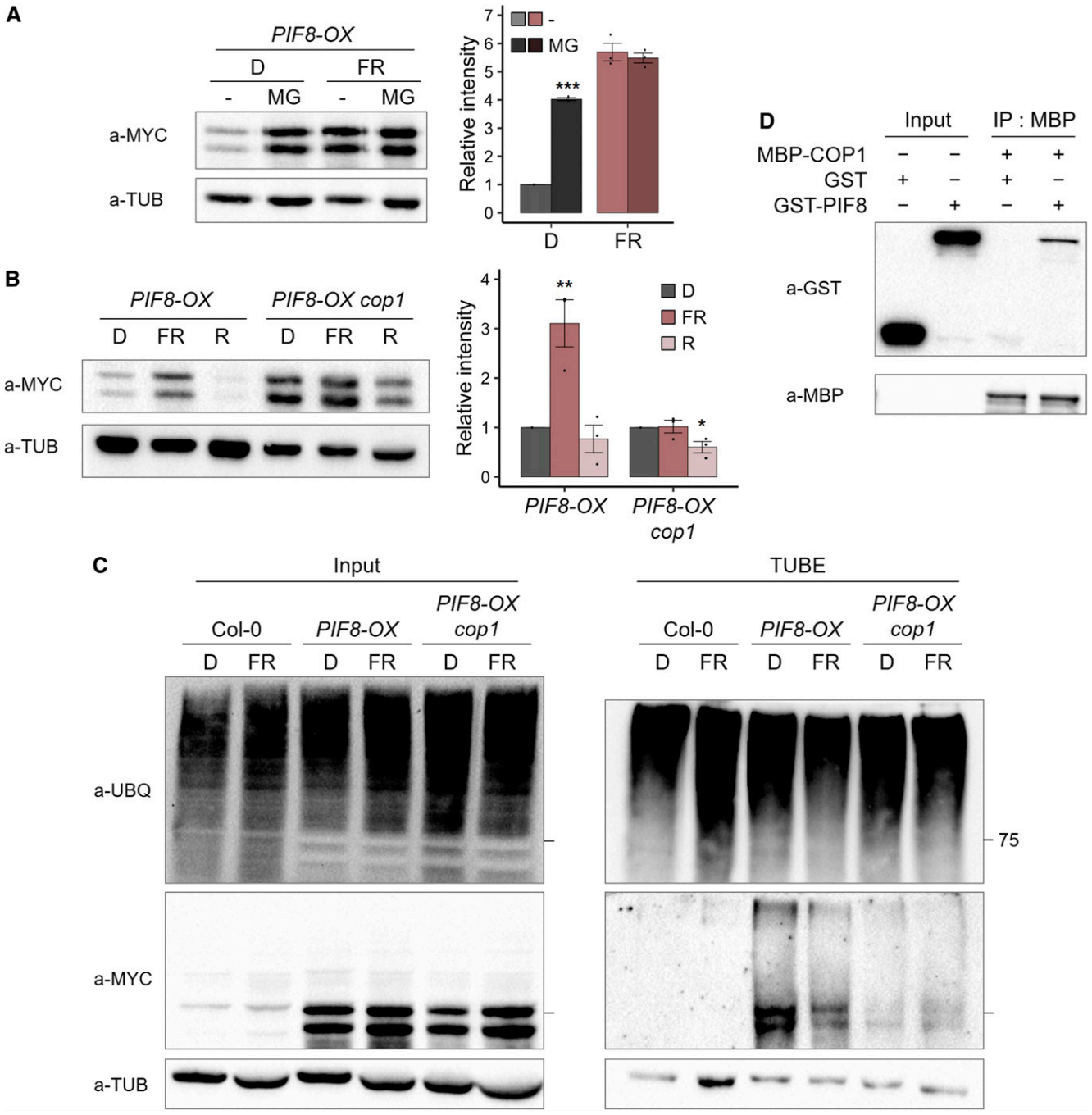

Figure 6. PIF8 Protein Is Degraded by COP1 in the Dark but Not in Far-Red Light.

(A) Stabilization of PIF8 protein by MG132 in the dark. Four-day-old etiolated *PIF8-OX* seedlings were treated with either 80 μM MG132 or the same amount of DMSO for 1 h in the dark and transferred either to the dark (D) or to far-red light (FR; 2.5 μmol m^{-2} s^{-1}) for 6 h. -, DMSO treatment; MG, MG132 treatment. Individual data points are indicated with dots. Asterisks indicate significant differences from the DMSO-treated values (***, $P < 0.001$; Student's *t* test). Error bars indicate SE ($n = 3$ biological replicates).

(B) Increased PIF8 protein level in the *cop1* mutant. *cop1*, *cop1-4* mutant; D, dark for 4 d; FR, far-red light (2.5 μmol m^{-2} s^{-1}) for 4 d. Asterisks indicate significant differences from the dark values (*, $P < 0.05$ and **, $P < 0.01$; Student's *t* test). Error bars indicate SE ($n = 3$ biological replicates).

(C) Preferential ubiquitination of PIF8 by COP1 in the dark. Seedlings were grown either in the dark (D) or in far-red light (FR; 2.5 μmol m^{-2} s^{-1}) for 4 d and treated with 80 μM MG132 for 12 h. Polyubiquitinated proteins were captured by TUBE. Input samples (Input) and the captured protein fractions (TUBE) were probed using an anti-ubiquitin antibody (a-UBQ), an anti-MYC antibody (a-MYC), and an anti-tubulin antibody (a-TUB).

(D) In vitro binding assay showing the direct interaction between PIF8 and COP1. Recombinant MBP-COP1 was mixed with recombinant GST-PIF8, and MBP-COP1 protein was pulled down with amylose resin. Coprecipitated GST-PIF8 was detected with a GST-specific antibody (a-GST), and MBP-COP1 was detected with an MBP-specific antibody (a-MBP).

2004; Jang et al., 2005; Yang et al., 2005; Zhou et al., 2014b). Thus, we examined whether COP1 degrades PIF8 in the dark. We generated a *PIF8-OX cop1* line by crossing *PIF8-OX* and the *cop1-4* mutant and measured its PIF8 protein levels in different light conditions. We noticed in *PIF8-OX cop1* mutant seedlings that PIF8 protein levels increase in the dark to levels similar to those grown in far-red light (Figure 6B), but this increase cannot be attributed to increased *PIF8* mRNA expression in dark-grown *PIF8-OX cop1* mutants (Supplemental Figure 6). These results support a role for COP1 in degrading PIF8 protein in the dark. Since phyA inhibits COP1/SPAs in far-red light (Osterlund and Deng, 1998; Chen et al., 2015; Sheerin et al., 2015), our results further suggest that phyA stabilizes PIF8 via its inhibition of COP1/SPAs in far-red light.

To further confirm that COP1 ubiquitinates and degrades PIF8 in the dark, we captured all ubiquitinated proteins from MG132-treated *PIF8-OX* and *PIF8-OX cop1* seedlings using the tandem ubiquitin binding entities (TUBEs) technique and measured the levels of captured PIF8 protein. Consistent with a selective degradation of PIF8 protein by COP1 in the dark, we found higher amounts of PIF8 captured by TUBE from *PIF8-OX* seedlings grown in the dark than in far-red light, whereas we found minimal capture of PIF8 from *PIF8-OX cop1* seedlings regardless of the light condition (Figure 6C). We could not attribute these different levels of PIF8 captured by TUBE to changes in overall ubiquitination, because we detected similar levels of ubiquitinated proteins with an anti-ubiquitin antibody (a-UBQ) in all seedlings regardless of light conditions. Together, these results support a role for COP1 in the preferential ubiquitination and degradation of PIF8 in the dark.

This preferential ubiquitination of PIF8 by COP1 in the dark but not in far-red light suggested that COP1 may directly interact with PIF8. To investigate this possibility, we performed in vitro binding assays using recombinant MBP-tagged COP1 and GST-tagged PIF8 (Figure 6D). We found that MBP-COP1 preferentially precipitates GST-PIF8 over GST alone, indicating that COP1 binds directly to PIF8. Together, our results support that COP1/SPAs directly interact with and ubiquitinate PIF8 in the dark.

phyA Sequesters PIF3 but Not PIF8 in Far-Red Light

Although both PIF3 and PIF8 proteins are present at significant levels, only *PIF8-OX* produces elongated hypocotyls in far-red light, suggesting that the presence of PIF8 protein is not the sole factor promoting hypocotyl elongation. According to previous studies, phyB inhibits PIF1, PIF3, and PIF4 not only by protein degradation but also by sequestering them from their target promoters (Park et al., 2012, 2018). Since phyA binds to PIF3 but not PIF8, phyA may inhibit PIF3 but not PIF8 by sequestration.

We first examined whether PIF8 binds directly to the G-box element (CACGTG), a canonical PIF binding sequence element. For in vitro DNA binding assays, we pulled down PIF8 protein with biotinylated promoter fragments containing G-box elements in the presence or absence of nonbiotinylated promoter fragments (Figures 7A and 7B). We confirmed the pull-down of PIF8 by biotinylated *PIL1* and *PIL2* promoter fragments (*PIL1pro* and *PIL2pro*; Figure 7B). This binding was disrupted by the addition of nonbiotinylated promoter fragments but not by the addition of promoter fragments with mutated G-boxes. As with PIF8, *PIL1pro* and *PIL2pro* can also pull-down PIF3 in vitro. These results indicate that PIF8, like PIF3, binds to G-box elements in vitro.

We next performed chromatin immunoprecipitation (ChIP) assays using *PIF3-OX* and *PIF8-OX* grown either in the dark or in far-red light. We found that PIF3 binds to both *PIL1pro* and *PIL2pro* in the dark, but its binding affinity falls dramatically in far-red light (Figure 7C). We found similar PIF3 protein levels in the dark and in prolonged far-red light, ruling out protein degradation as the cause of this reduced binding in far-red light (Figure 5A). We also continued to observe reduced PIF3 binding to its target promoters in far-red light compared with the dark even as we inhibited residual PIF3 protein degradation with MG132 (Figure 7D). Unlike what we observed with MG132 treatment, in the presence of *phyA* mutation, we observed similar levels of PIF3 binding to its target promoters in the dark and in far-red light (Figure 7E). This suggests that phyA sequesters PIF3 from its target promoters in far-red light. In the same ChIP assays, however, we observed much stronger binding of PIF8 to its target promoters in far-red light than in the dark (Figure 7C). This stronger binding in far-red light can be attributed in part to higher PIF8 protein levels in far-red light. This was made clear when we found similar levels of PIF8 binding in the dark and in far-red light after equalizing PIF8 protein levels via MG132 treatment or *phyA* mutation (Figures 7D and 7E). Thus, phyA inhibits PIF3 but not PIF8 by sequestering it in far-red light. Furthermore, this lack of sequestration by phyA combined with the elevated levels of PIF8 protein in far-red light contributes to the role of PIF8 but not PIF3 in promoting hypocotyl elongation in far-red light.

DISCUSSION

Here, we characterized the most poorly studied member of the PHYTOCHROME INTERACTING FACTOR protein family, PIF8, whose putative orthologs are conserved in plant species as diverse as tomato and rice. PIF8 possesses a bHLH domain and a highly conserved APB motif, but it does not have a conserved APA motif. Consistent with its motif composition, PIF8 binds to G-box elements in its target gene promoters and interacts preferentially with the Pfr form of phyB but only very weakly, if at all, with that of phyA. Interestingly, PIF8 is distinct from the other more well-characterized Arabidopsis PIFs in its protein stability pattern and functional roles in different light conditions. First, PIF8 represses photomorphogenic development in far-red but not in red light; it inhibits phyA-induced seed germination, suppression of hypocotyl elongation, cotyledon opening, and suppression of hypocotyl negative gravitropism in far-red light, but it does not inhibit phyB-induced light responses in red light. Second, PIF8 protein is more stable in far-red light than in the dark or in red light, whereas other PIFs, PIF3 for example, are more stable in the dark than in far-red and red light. This pattern of PIF8 accumulation is accomplished by the combination of COP1/SPAs-induced degradation of PIF8 in the dark, phyA-induced inhibition of COP1/SPAs in far-red light, and the degradation of PIF8 by phyB in red light. Together, our results indicate that PIF8 is a genuine PIF that inhibits phyA-mediated far-red light responses (Figure 8).

The exact molecular mechanism by which PIF8 inhibits phyA- and not phyB-mediated light responses is not fully clear. PIF8 binds the promoters of PIF target genes and activates their mRNA

expression (Figure 7; Supplemental Figure 3), suggesting that PIF8, like PIF3, inhibits light responses via its role as a transcription factor. The selective stabilization of PIF8 combined with its resistance to being sequestered by phyA in far-red light would make PIF8 more active in far-red than in red light, thus biasing its action toward the inhibition of phyA-mediated light responses. It is unclear, however, whether the far-red light specificity of PIF8 is due solely to increased transcription factor activity in far-red light. Comparisons of the transcriptome- and genome-wide binding sites of PIF8 and PIF3 would allow us to confirm whether they bind similar target genes despite their preferential inhibition of phyA- or phyB-mediated light responses, respectively.

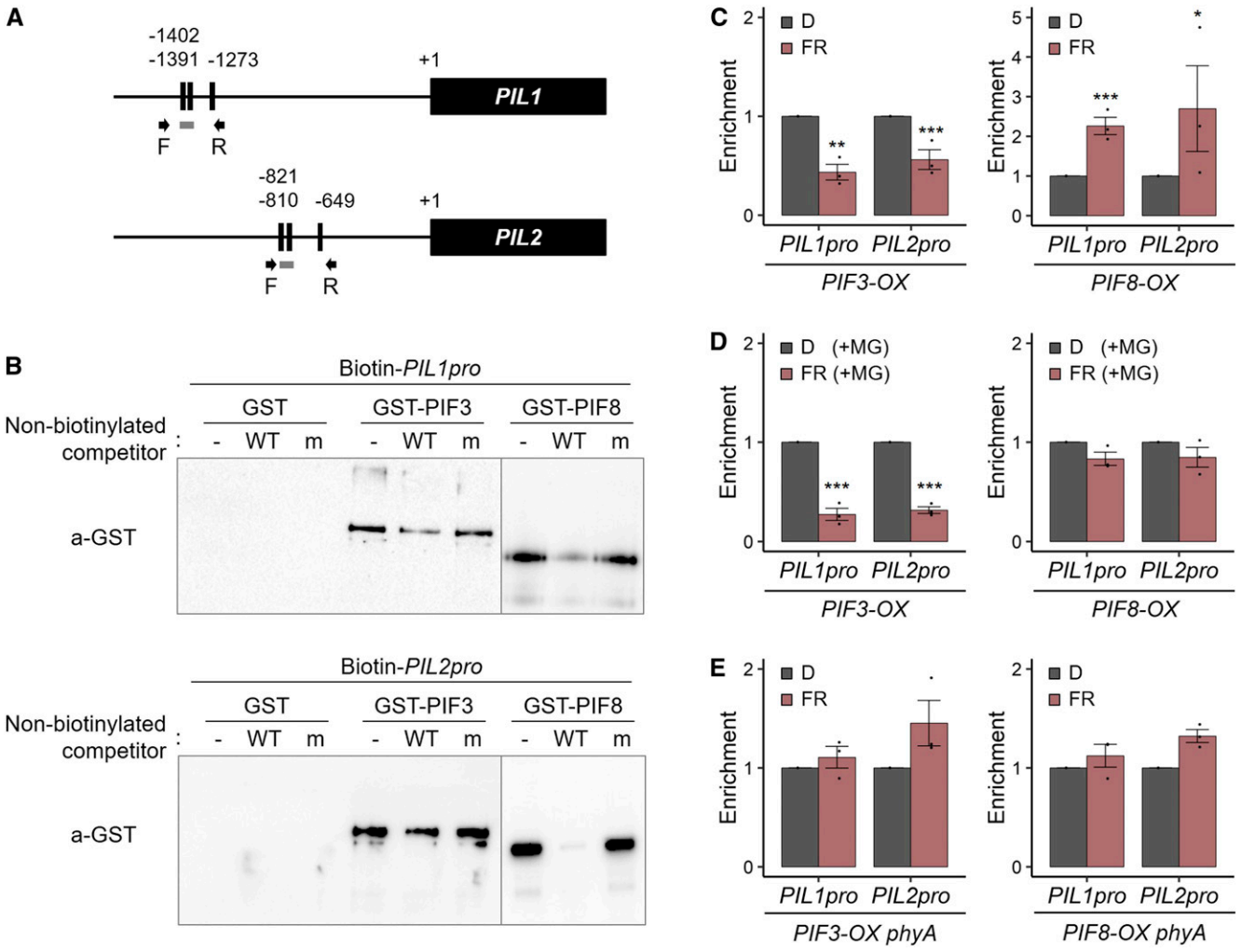

Figure 7. PIF8 Binds to G-Box Elements and Promoters of PIF Target Genes.

(A) Diagrams of the *PIL1* and *PIL2* promoters. Black lines, promoters; black bars, G-box elements; black arrows, forward (F) and reverse (R) primers used in ChIP-qPCR; gray lines, promoter fragments used in in vitro DNA binding assays. Numbers indicate the distance in base pairs from the translation start site.

(B) Binding of PIF8 to G-box elements in vitro. For in vitro DNA binding assays, biotin-labeled *PIL1* or *PIL2* promoter fragments possessing G-box elements (*PIL1pro* or *PIL2pro*) were mixed with GST-tagged PIF proteins in the presence or absence of nonbiotinylated promoter fragments (competitor). After precipitation with streptavidin resin, coprecipitated proteins were detected with an anti-GST antibody (a-GST). -, non-treated; m, nonbiotinylated promoter fragments with mutated G-box elements; WT, nonbiotinylated promoter fragments with wild-type G-box elements.

(C) Increased in vivo binding of PIF8 to *PIL1pro* and *PIL2pro* in far-red light. Transgenic seedlings expressing either MYC-tagged PIF8 (*PIF8-OX*) or MYC-tagged PIF3 (*PIF3-OX*) were grown in different light conditions for 4 d for ChIP assays. D, dark; FR, far-red light (2.5 μmol m^{-2} s^{-1}). Enrichment in the dark was set to 1. Individual data points are indicated with dots. Asterisks indicate significant differences from the enrichment in the dark (*, $P < 0.05$; **, $P < 0.01$; and ***, $P < 0.001$; Student's *t* test). Error bars indicate SE ($n = 3$ biological replicates).

(D) Similar in vivo binding of PIF8 but not PIF3 to *PIL1pro* and *PIL2pro* in different light conditions in the presence of MG132. Seedlings were treated with 80 μM MG132 for 12 h before fixation for ChIP assays. Enrichment in the dark was set to 1. Individual data points are indicated with dots. Asterisks indicate significant differences from the enrichment in the dark (***, $P < 0.001$; Student's *t* test). Error bars indicate SE ($n = 3$ biological replicates).

(E) Similar in vivo binding of both PIF8 and PIF3 to *PIL1pro* and *PIL2pro* in different light conditions in *phyA* mutants. Enrichment in the dark was set to 1. Individual data points are indicated with dots. Error bars indicate SE ($n = 3$ biological replicates).

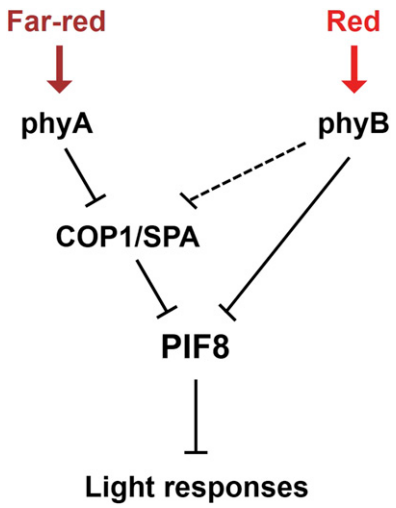

Figure 8. Diagram Showing the Regulation of PIF8 by phyA and phyB.

PIF8, like other PIFs, binds to G-box elements in target promoters and regulates target gene expression, leading to the suppression of light responses. PIF8 activity is disabled both in the dark, because COP1/SPAs ubiquitinate and degrade PIF8 protein in the dark, and in red light, because phyB interacts with and promotes PIF8 protein degradation in red light. Since phyA does not interact with PIF8 protein, however, phyA does not degrade or sequester PIF8 in far-red light. Instead, phyA interacts with and inhibits COP1/SPAs, stabilizing PIF8 protein in far-red light. This stabilized PIF8 then regulates target gene expression, repressing light responses, including inhibition of hypocotyl elongation and seed germination in far-red light. The dotted bar-headed line indicates inhibition of COP1/SPAs by phyB, the effect of which is overridden by phyB's promotion of PIF8 protein degradation in red light. The solid bar-headed lines indicate the inhibitory regulation.

PIF8 is an Arabidopsis PIF possessing a bHLH motif and an APB motif but no APA motif. Two tomato PIF8 homologs (Sl-PIF8a and Sl-PIF8b) and a rice homolog (Os-PIF8) also possess a bHLH motif and an APB motif but no APA motif (Supplemental Figure 1). This motif composition is similar to that of PIF2, PIF4, PIF5, PIF6, and PIF7 but different from that of PIF1 and PIF3, which possess both the APA and APB motifs (Leivar and Quail, 2011). The tomato and rice PIFs and PILs that cluster with Arabidopsis PIF1 and PIF3 (i.e., Sl-PIF1a, Sl-PIF1b, Sl-PIF3, and Os-PIL15) also possess both APA and APB motifs, whereas tomato and rice PIFs and PILs that cluster with Arabidopsis PIF4, PIF5, PIF7, and PIF8 (i.e., Sl-PIF4/PIF5, Sl-PIF7a, Sl-PIF7b, Sl-PIF8a, Sl-PIF8b, and Os-PIF8) do not have APA motifs (Figure 1B; Nakamura et al., 2007; Zhou et al., 2014a; Rosado et al., 2016; Lee and Choi, 2017; Ji et al., 2019). Thus, the absence of an APA motif is one of the most distinguishing features of PIF8 and its homologs.

The motif composition of PIF8 partly explains its molecular properties. First, PIF8's ability to bind to G-box motifs in vitro and promoters containing G-box motifs in vivo can be attributed to its bHLH motif (Figure 7). Studies have shown that the bHLH motifs of Arabidopsis PIFs bind to specific sequence elements including G-boxes (CACGTG) and PIF binding E-boxes (ACATG; Martínez-García et al., 2000; Huq and Quail, 2002; Huq et al., 2004; Oh et al., 2007, 2009; Kim et al., 2008; Leivar et al., 2008b; Hornitschek et al., 2009, 2012; Kidokoro et al., 2009; Li, 2012; Zhang et al., 2013; Li et al., 2014; Pfeiffer et al., 2014). Similarly, PIFs in other plant species including Sl-PIF1, Sl-PIF3, Os-PIL13, and Os-PIL14 also bind to G-boxes or promoters containing G-box or PIF binding E-box elements (Todaka, 2012; Cordeiro et al., 2016; Llorente et al., 2016; Sakuraba et al., 2017; Wang et al., 2018).

Second, the presence of an APB motif but not an APA motif likely explains why PIF8 binds to phyB but only very weakly, if at all, to phyA. In previous studies, Arabidopsis PIFs with an APB motif bind to phyB, whereas PIF4, PIF5, and PIF7, which lack an APA motif, either do not bind to phyA or bind only weakly (Huq and Quail, 2002; Huq et al., 2004; Shen et al., 2007; Leivar et al., 2008b; Leivar and Quail, 2011; Lee and Choi, 2017). Similarly, APA-containing PIFs in other plant species including maize (*Zea mays*; i.e., Zm-PIF1, Zm-PIF2, and Zm-PIF3) bind to phyA, while APB-containing PIFs including rice Os-PIL14, Os-PIL15, and Os-PIL16 and maize Zm-PIF1 through Zm-PIF6 bind to phyB (Cordeiro et al., 2016; He et al., 2016; Kumar et al., 2016; Gao et al., 2019; Xie et al., 2019). This is consistent with the APA and APB motifs of PIFs being necessary for binding to phyA and phyB, respectively. APA and APB motifs, however, do not seem to be the sole determining factor for a PIF's ability to interact with either phyA or phyB. In our experiments, PIF5, although lacking an APA motif, binds to the Pfr form of phyA (Supplemental Figure 7). PIF4, which also lacks an APA motif, does not bind to phyA in vitro. Rice Os-PIL13, which has an APB motif, does not interact with rice phyB (Todaka et al., 2012). Since in vitro binding assays can be influenced by experimental conditions, further experimental verification will be necessary to conclude whether the APA and APB motifs are necessary and sufficient for PIF interactions with phyA and phyB, respectively.

Third, PIF8's lack of an APA motif only partly accounts for its light-dependent degradation. Previous studies have implicated the APA motif in phyA-induced PIF protein degradation in far-red light and the APB motif in phyB-induced PIF protein degradation in red light. Consistent with this, PIF1 and PIF3, which possess both the APA and APB motifs, are degraded both in red and far-red light, whereas PIF4 and PIF5, which possess the APB motif but not the APA motif, are degraded in red light and only weakly degraded in far-red light (Bauer et al., 2004; Park et al., 2004; Al-Sady et al., 2006; Oh et al., 2006; Shen et al., 2007, 2008; Lorrain et al., 2008). Consistent with its APB motif, red light-induced degradation of PIF8 protein is dependent on phyB. Curiously, however, rather than being degraded by phyA, PIF8 protein is stabilized by phyA in far-red light. This degradation pattern is distinct from that of PIF1 and PIF3 and from that of PIF4 and PIF5. It is also different from that of PIF2, which is stabilized in red light, and that of PIF7, which is not degraded in red light (Leivar et al., 2008b; Luo et al., 2014). Thus, although the APA and APB motifs are necessary for phyA- and phyB-dependent PIF degradation, respectively, the presence of an APA or APB motif cannot be considered the only factor determining phyA- or phyB-dependent PIF degradation.

Our data indicate that COP1 also shapes the PIF8 protein degradation pattern in different light conditions. PIF8 protein is polyubiquitinated and degraded by the 26S proteasome in the dark, whereas it is stabilized in a phyA-dependent manner in far-red light. Because PIF8 does not directly interact with phyA, this phyA-dependent stabilization of PIF8 protein in far-red light must

occur through interaction with another protein. Our data show that COP1 directly interacts with and ubiquitinates PIF8, whereas phyA stabilizes PIF8 in far-red light by inhibiting COP1. According to previous studies, phyA inhibits COP1/SPAs either by excluding COP1 from the nucleus (Osterlund and Deng, 1998), by disrupting the COP1/SPA complex (Sheerin et al., 2015), or by degrading SPA proteins (Balcerowicz et al., 2011; Chen et al., 2015). Since COP1/SPAs are light-blind ubiquitin E3 ligases, it seems more likely that COP1/SPAs would ubiquitinate PIF8 protein regardless of the light condition. In far-red light, however, phyA's inhibition of COP1/SPAs inhibits the COP1-dependent ubiquitination of PIF8, resulting in higher accumulation of PIF8 in far-red light than in the dark. Blue light also inhibits COP1/SPAs via cryptochromes and phyA (Lian et al., 2011; Liu et al., 2011; Sheerin et al., 2015). Consistently, PIF8 protein is stabilized in blue light (Supplemental Figure 8). PIF8 protein levels in red light are also higher in *cop1* mutant seedlings than in the wild type, suggesting that phyB also inhibits the action of COP1/SPAs on PIF8. However, PIF8 protein is still degraded in *cop1* mutant seedlings grown in red light (Figure 6B), indicating that the degradation of PIF8 by phyB can override phyB-mediated inhibition of COP1/SPAs in red light. Together, these results suggest that PIF8's light-dependent degradation pattern is determined by a combination of COP1/SPA-mediated degradation of PIF8 in the dark, phyA-mediated inhibition of COP1/SPAs leading to the stabilization of PIF8 in far-red light, and phyB-mediated degradation of PIF8 in red light.

COP1 also regulates the stability of other PIFs, but not all PIFs are unilaterally degraded by COP1/SPAs. PIFs can either be stabilized or destabilized depending on the identity of the PIF and on light conditions. PIF1, PIF3, PIF4, and PIF5 are stabilized by COP1 in the dark (Bauer et al., 2004; Pham et al., 2018a, 2018b). Although the mechanism by which this PIF stabilization occurs is not fully understood, PIF3 stabilization by COP1 can be attributed to COP1's inhibition of the BIN2 protein kinase, which itself phosphorylates and destabilizes PIF3 (Ling et al., 2017). Upon prolonged light exposure, however, the stability of PIF1, PIF3, PIF4, and PIF5 is not regulated by COP1. Very shortly after the transition from dark to light, PIF1 and PIF5 are destabilized by the COP1/SPA complex (Shen et al., 2008; Zhu et al., 2015; Pham et al., 2018b). Among the other less-characterized PIFs, PIF2 is destabilized by COP1 in the dark but not in red, far-red, and blue light (Luo et al., 2014). At this point, it is unclear what determines these various COP1/SPAs-associated PIF degradation patterns.

Our data indicate that PIF8 promotes hypocotyl elongation in blue, far-red, or mixed blue and far-red light but not in red light (Figure 3; Supplemental Figure 8). This PIF8 activity is quite different from those of the better-characterized PIFs including PIF1, PIF3, PIF4, PIF5, and PIF7, which promote hypocotyl elongation in red light but either not at all in far-red light (PIF3 and PIF7) or very weakly in far-red light (PIF1, PIF4, and PIF5; Huq and Quail, 2002; Kim et al., 2003; Fujimori et al., 2004; Oh et al., 2004; Khanna et al., 2007; Leivar et al., 2008b; Castillon et al., 2009; Lorrain et al., 2009; Kunihiro et al., 2010; Ma et al., 2016). PIF8 is also different from PIF2, which weakly inhibits hypocotyl elongation in red, far-red, and blue light (Luo et al., 2014). These different light-specific activities of the various PIFs are not merely due to light-dependent PIF degradation. Rather, these functional differences arise from a combination of factors including light-dependent PIF degradation and light-dependent PIF sequestration by phytochromes and other proteins such as HFR1 and DELLA (de Lucas et al., 2008; Feng et al., 2008; Hornitschek et al., 2009; Lorrain et al., 2009; Park et al., 2012; Shi et al., 2013). Such light-specific PIF8 activities should mitigate excessive phyA-mediated light responses in conditions enriched with far-red and blue light. The ecological conditions in which PIF8 plays a key role must still be identified.

METHODS

Plant Materials and Growth Conditions

Arabidopsis (*Arabidopsis thaliana*) plants were grown in a growth room under long-day conditions (16 h of white light/8 h of dark; white light, 100 μmol m^{-2} s^{-1}; LED light bulb) at 22°C for general growth and harvesting purposes. All plants were of the Col-0 background. The *pif8-1* mutant (*CS429358*) was obtained from the ABRC. The *pif8-2* mutant was generated via CRISPR-CAS9 (single guide RNA, CCAAACTGTCACATC GATGATAC; Park et al., 2015; Kim et al., 2016a; Labun et al., 2016). The mutation caused by the insertion of a thymidine residue in the *PIF8* gene was confirmed by sequencing. The following mutants were obtained from the ABRC: *pif4*, *CS101616*; *pif5*, *CS2103235*; *pif7*, *CS71656*; and *hfr1*, *SALK_037727C*. *PIF8-OX* was generated by cloning the *PIF8* coding region into the *pkHTM* vector and introducing it into wild-type Col-0 by *Agrobacterium tumefaciens*-mediated floral dip transformation (Clough and Bent, 1998; Oh et al., 2004). The sequences of all the primers used in this study are listed in Supplemental Table 1.

Phylogenetic and Expressional Clustering Analyses

For the PIF8 phylogenetic clustering analysis, putative PIF ortholog sequences were retrieved by homology search of OrthoDB and Phytozome in conjunction with literature studies (Nakamura et al., 2007; Goodstein et al., 2012; Rosado et al., 2016; Kriventseva et al., 2019). The amino acid sequences were aligned with MUSCLE using the default settings, and a phylogenetic tree was inferred by applying the maximum likelihood method with 500 bootstrap repeats using MEGA X (Kumar et al., 2018). For the *PIF8* expression clustering analysis, the expression levels of each *PIF* gene in various tissues and developmental stages were retrieved from the Klepikova Arabidopsis Atlas eFP browser (Klepikova et al., 2016). The expression patterns for the *PIF* genes were analyzed by hierarchical clustering with Multiple Experiment Viewer (distance metric, Pearson correlation; linkage method, average linkage clustering; Saeed et al., 2003). The sequence alignment and tree file are provided in Supplemental Files 1 and 2, respectively.

Analysis of Plant Phenotypes

Hypocotyl Elongation

Seeds were surface-sterilized with a sterilization solution containing 0.4% (w/v) sodium hypochlorite and 0.02% (v/v) Triton X-100. The sterilized seeds were then spotted onto Murashige and Skoog (MS) agar plates containing half-strength MS medium, 0.05% (w/v) MES, and 0.8% (w/v) phytoagar (pH 5.7). Plates were stratified for 3 d in the dark at 4°C and transferred to white light (50 μmol m^{-2} s^{-1}) for 6 h at 22°C for germination induction. The plates were then transferred to red (660 nm, 15 μmol m^{-2} s^{-1}), far-red (730 nm, 1 μmol m^{-2} s^{-1}), blue (450 nm, 5.2 μmol m^{-2} s^{-1}), or mixed light (blue + far-red; blue, 1.2 μmol m^{-2} s^{-1}; far-red, 1.5 μmol m^{-2} s^{-1}) and grown for 4 d. The seedlings were then laid out on plates for photographs, and the hypocotyl lengths were measured with the Multi

Gauge software (Fuji Film). ANOVA results are provided in Supplemental Table 2.

Shade Response

Surface-sterilized seeds were stratified, and germination was induced as described above. The seedlings were then grown in high red:far-red light (red, 8 μmol m^{-2} s^{-1}; far-red, 0.4 μmol m^{-2} s^{-1}; blue, 12 μmol m^{-2} s^{-1}; red:far-red ratio = 20) for 4 d. They were then either kept in high red:far-red light (normal) or transferred to low red:far-red light (shade; red, 8 μmol m^{-2} s^{-1}; far-red, 55 μmol m^{-2} s^{-1}; blue, 12 μmol m^{-2} s^{-1}; red:far-red ratio = 0.15) for an additional 3 d before their hypocotyl lengths were measured.

Hypocotyl Negative Gravitropism

Surface-sterilized seeds were stratified, and germination was induced as described above. The plates were then placed vertically in growth chambers, and the seedlings were grown under red (15 μmol m^{-2} s^{-1}) or far-red (1 μmol m^{-2} s^{-1}) light for 4 d. If the shoot apex was within $\pm$45° from the vertical line, the seedlings were regarded as standing (Kim et al., 2016c). The standing rate was then calculated as (number of standing seedlings)/(number of total seedlings) $\times$ 100 (%).

Amyloplast Staining

For amyloplast visualization, seedlings were fixed with a fixation solution (5% [v/v] formaldehyde, 5% [v/v] acetic acid, and 45% [v/v] ethanol) overnight at 4°C, washed in 100% ethanol, and stained with I_2-KI solution (2% [w/v] iodine, 5% [w/v] potassium iodide, and 20% [v/v] trichloroacetic acid) for 1 min Kim et al., 2016c. The stained seedlings were briefly washed with a destaining solution (50% [v/v] trichloroacetic acid, 25% [v/v] phenol, and 25% [v/v] lactate) before observation with a light microscope.

Germination

For the germination assays, 70 seeds of each genotype were surface-sterilized and spotted onto MS agar plates containing 1% strength MS medium, 0.05% (w/v) MES, and 0.8% (w/v) phytoagar (pH 5.7) within 1 h of the start of sterilization. For the phyA-mediated germination assays, spotted seeds were irradiated with a far-red light pulse (2.5 μmol m^{-2} s^{-1}) for 5 min, incubated for 2 d in the dark at 22°C, irradiated for the indicated number of hours with far-red light (2.5 μmol m^{-2} s^{-1}), and further incubated for 4 d in the dark at 22°C. For the phyB-mediated germination assays, spotted seeds were irradiated with a far-red light pulse (2.5 μmol m^{-2} s^{-1}) for 5 min with or without a follow-up red light pulse (15 μmol m^{-2} s^{-1}) for 5 min and then incubated for 4 d in the dark at 22°C. Seeds with protruding radicles were counted as germinated seedlings.

RNA Expression Analysis

Seedlings grown on MS agar plates with an additional supplement of 1% (w/v) Suc in the indicated conditions were collected and ground in liquid nitrogen. Total RNA was extracted using the Spectrum Plant Total RNA Kit (STRN250, Sigma-Aldrich). For the expression analysis, 2 μg of isolated RNA was reverse transcribed to cDNA with M-MLV Reverse Transcriptase (M1701, Promega), and the expression level of each gene was determined by quantitative real-time PCR with a set of specific primers and the TOPreal qPCR 2X PreMIX (RT500, Enzynomics) in the CFX Connect Real-Time PCR Detection System (Bio-Rad Laboratories). All the values were normalized with respect to the values of *PP2A*. All expression analysis was performed in three biological replicates using different seedling samples. The sequences of all the primers used in this study are listed in Supplemental Table 1.

Protein-Protein Interaction Assays

In Vitro Interaction Assays

Recombinant proteins were purified from *Escherichia coli* strain BL21-CodonPlus-RIL cell lines with the exception of phyA and phyB, which were purified from LMG194 lines (Gambetta and Lagarias, 2001). For the in vitro binding assays, GST-tagged PIF proteins bound to Glutathione Sepharose 4B resins (17075601, GE Healthcare) were mixed with MYC-tagged phytochrome proteins pretreated for 5 min with far-red light (2.5 μmol m^{-2} s^{-1}) or red light (15 μmol m^{-2} s^{-1}) to generate the Pr or Pfr form, respectively. These were then incubated in a binding buffer (50 mM Tris-HCl, 1 mM EDTA, 150 mM NaCl, 0.1% [v/v] Triton X-100, 0.05% [w/v] sodium deoxycholate, and 10% [v/v] glycerol, pH 7.5) with gentle rotation at 4°C in the dark for 2 h. After this, the glutathione resins were precipitated, and the coprecipitated phytochromes were detected with an anti-MYC antibody. For the in vitro binding assay between PIF8 and COP1, MBP-tagged COP1 proteins bound to Amylose Resins (E8021, New England Biolabs) were mixed with GST-tagged PIF8 proteins and incubated in binding buffer with gentle rotation at 4°C for 2 h. After the precipitation of the amylose resins, the coprecipitated PIF8 proteins were detected with an anti-GST antibody.

Semi-in Vivo Interaction Assays

Four-day-old etiolated seedlings expressing FLAG-tagged phytochromes (*PHYA-FLAG*, *PHYApro:PHYA-NLS-FLAG phyA phyB*; *PHYB-FLAG*, *35Spro:PHYB-NLS-FLAG phyA phyB*) were ground in liquid nitrogen and dissolved in a semi-immunoprecipitation buffer (50 mM Tris-HCl, 150 mM NaCl, 0.1% [v/v] Triton X-100, 10% [v/v] glycerol, 1 mM PMSF, and 1$\times$ protease inhibitor cocktail, pH 7.5). After removing the cell debris by centrifugation at 15,810*g* for 10 min at 4°C, the supernatant fractions were mixed with recombinant GST-tagged PIF proteins bound to Glutathione Sepharose 4B resins. These mixtures were treated with either 5 min of far-red light (2.5 μmol m^{-2} s^{-1}) or red light (15 μmol m^{-2} s^{-1}) to generate the Pr or Pfr phytochrome form, respectively. These were then incubated with gentle rotation at 4°C in the dark for 2 h. After the incubation, the glutathione resins were precipitated. The coprecipitated phytochromes were detected with an anti-FLAG antibody.

In Vivo Interaction Assays (Coimmunoprecipitation Assays)

Four-day-old etiolated seedlings expressing MYC-tagged PIFs with or without FLAG-tagged phyB were treated either with far-red light (2.5 μmol m^{-2} s^{-1}) or red light (15 μmol m^{-2} s^{-1}) for 30 min to generate the Pr or Pfr phytochrome form, respectively. The seedlings were collected, ground in liquid nitrogen, and dissolved in an immunoprecipitation buffer (100 mM NaH_2PO_4, 100 mM NaCl, 0.1% [v/v] Nonidet P-40, 2 mM PMSF, 80 μM MG132, and 1$\times$ protease inhibitor cocktail, pH 7.8). After removing the cell debris by centrifugation at 15,810*g* for 10 min at 4°C, the supernatant fractions were incubated with a-MYC (no. 2276, Cell Signaling Technology) with gentle rotation at 4°C overnight in the dark. After the overnight incubation, Protein A Agarose (no. 20333, Pierce Biotechnology) was added, and the sample was incubated for 2 h and then precipitated. The resulting coimmunoprecipitated phytochromes were detected with an anti-PHYA antibody for endogenous phyA or an anti-FLAG antibody for PHYB-FLAG.

Immunoblot Analysis

Seedlings grown under the indicated conditions were collected and ground in liquid nitrogen. The resulting powders were dissolved in denaturing buffer (120 mM NaH_2PO_4, 8 M urea, and 10 mM Tris-HCl, pH 8.0) and centrifuged at 15,810*g* for 10 min at 4°C. The supernatant fractions were boiled with SDS sample buffer, and the protein levels were determined by immunoblot analysis using the following antibodies: a-MYC (sc-789, Santa Cruz Biotechnology), a-TUB (T9026, Sigma-Aldrich), a-FLAG (F2555,

Sigma-Aldrich), a-GST (sc-138, Santa Cruz Biotechnology), a-MBP (sc-809, Santa Cruz Biotechnology), a-UBQ (no. 3936, Cell Signaling Technology), a-PHYA (AS07 220, Agrisera), goat anti-rabbit IgG-HRP (sc-2004, Santa Cruz Biotechnology), mouse anti-rabbit IgG-HRP (sc-2357, Santa Cruz Biotechnology), and goat anti-mouse IgG-HRP (LF-SA8001, AbFrontier). Luminescence was detected using the ChemiDoc XRS+ System (Bio-Rad Laboratories) after reacting with EzWestLumiOne (WSE-7110, ATTO) or Clarity Western ECL Substrate (no. 1705060, Bio-Rad Laboratories). Band intensities were quantified using Image Lab Software (Bio-Rad Laboratories). Relative intensities were determined by the band intensity of the PIF protein bands relative to the band intensity of the tubulin band. This analysis was performed on three biological replicates with each using different seedling samples.

TUBE Assay

Four-day-old seedlings grown either in the dark or in far-red light (2.5 μmol m^{-2} s^{-1}) were pretreated with 80 μM MG132 for 12 h. The seedlings were collected and ground in liquid nitrogen. The resulting powders were then mixed with TUBE pull-down buffer (100 mM NaH_2PO_4, 100 mM NaCl, 0.1% [v/v] Nonidet P-40, 2 mM PMSF, 80 μM MG132, 1× protease inhibitor cocktail, and 20 μM PR-619, pH 7.8), and the cellular debris was removed by two rounds of centrifugation at 15,810*g* at 4°C. Agarose-TUBE (UM402, Lifesensors) was added to the clear supernatants and incubated with gentle rotation in the dark at 4°C overnight. The captured fractions were then washed with TUBE pull-down buffer three times, and ubiquitinated MYC-tagged PIF8 was detected with an anti-MYC antibody.

In Vitro DNA Binding Assays

Biotin-labeled double-stranded oligonucleotides complementary to the *PIL1* and *PIL2* promoters (400 ng each) were bound to Streptavidin Agarose Resin (20347, Thermo Fisher Scientific) and equilibrated with TKNG buffer (20 mM Tris-HCl, 150 mM KCl, 1 mM EDTA, 0.5% [v/v] Nonidet P-40, and 15% [v/v] glycerol, pH 8.0). Then, 800 ng of GST-PIF3 or GST-PIF8 protein was added and the samples were incubated in the presence of 1 μg of poly dI-dC (deoxyinosinic-deoxycytidylic; 118578-37-3, Sigma-Aldrich) and 1 μg of BSA at 4°C for 2.5 h. If indicated, the nonbiotinylated double-stranded *PIL1* and *PIL2* promoter oligonucleotides with the wild-type sequence or a G-box mutated sequence were coincubated. Resin-bound fractions were washed with TKNG buffer three times, and the remaining bound GST-PIF proteins were detected with an anti-GST antibody. All oligonucleotide sequences used in the in vitro DNA pull-down assays are listed in Supplemental Table 1.

ChIP

ChIP experiments were performed as previously described with slight modifications (Gendrel et al., 2002; Park et al., 2018). One gram of 4-d-old seedlings grown either in the dark or in far-red light (2.5 μmol m^{-2} s^{-1}) was cross-linked with 1% (v/v) formaldehyde solution by vacuum infiltration (5 min on, break, 5 min on) under green light. If indicated, seedlings were pretreated with 80 μM MG132 for 12 h before cross-linking. After being ground in liquid nitrogen, the chromatin fractions were isolated usingSuc gradients and sonicated for four cycles (30 s on, 30 s off) in a nuclei lysis buffer (50 mM Tris-HCl, 10 mM EDTA, 1% (w/v) SDS, 1 mM PMSF, 1× protease inhibitor cocktail, and 80 μM MG132, pH 8.0) using a Bioruptor Standard (Diagenode). After centrifugation at 15,810*g* at 4°C, the supernatant fractions were diluted with ChIP dilution buffer (1.1% [v/v] Triton X-100, 1.2 mM EDTA, 16.7 mM Tris-HCl, 167 mM NaCl, 1 mM PMSF, 1× protease inhibitor cocktail, and 80 μM MG132, pH 8.0). After incubation with a-MYC (no. 2276, Cell Signaling Technology) overnight at 4°C, Protein A Agarose/Salmon Sperm DNA (16-157, Merck Millipore) was added and incubated for 2 h. The resin-bound fractions were washed and eluted with elution buffer (1% [w/v] SDS and 0.1 M $NaHCO_3$) at 65°C for 30 min. The eluted fractions were then reverse cross-linked with NaCl (final concentration 0.2 M) at 65°C overnight. The fractions were then treated with 0.024 mg of Proteinase K (no. 25530049, Invitrogen) for 1 h at 45°C. The precipitated DNAs were purified using QIAquick PCR Purification Kits (28106, Qiagen) and used for quantitative real-time PCR with iQ SYBR Green Supermix (no. 1708882, Bio-Rad Laboratories). All the values were normalized with respect to their input values. All ChIP analysis was performed on three biological replicates using different seedling samples. The sequences of all the primers used in this study are listed in Supplemental Table 1.

Accession Numbers

Sequence data from this article can be found in the GenBank/EMBL libraries, Rice Annotation Project, and Sol Genomics Network data library under the following accession numbers: *PIF1* (*AT2G20180*), *PIF2/PIL1* (*AT2G46970*), *PIF3* (*AT1G09530*), *PIF4* (*AT2G43010*), *PIF5* (*AT3G59060*), *PIF6* (*AT3G62090*), *PIF7* (*AT5G61270*), *PIF8* (*AT4G00050*), *HFR1* (*AT1G02340*), *COP1* (*AT2G32950*), *PHYA* (*AT1G09570*), *PHYB* (*AT2G18790*), *PP2A* (*AT1G13320*), *Sl-PIF1a* (*Solyc09g063010*), *Sl-PIF1b* (*Solyc06g008030*), *Sl-PIF3* (*Solyc01g102300*), *Sl-PIF4/PIF5* (*Solyc07g043580*), *Sl-PIF7a* (*Solyc03g115540*), *Sl-PIF7b* (*Solyc06g069600*), *Sl-PIF8a* (*Solyc01g090790*), *Sl-PIF8b* (*Solyc10g018510*), *Os-PIL11* (*LOC_Os12g41650*), *Os-PIL12* (*LOC_Os03g43810*), *Os-PIL13* (*LOC_Os03g56950*), *Os-PIL14* (*LOC_Os07g05010*), *Os-PIL15* (*LOC_Os01g18290*), *Os-PIL16* (*LOC_Os05g04740*), and *Os-PIF8* (*LOC_Os10g40740*).

Supplemental Data

Supplemental Figure 1. Sequence alignment of PIF8 orthologs from *Arabidopsis thaliana*, *Solanum lycopersicum*, and *Oryza sativa* (supports Figure 1).

Supplemental Figure 2. Expression pattern clustering for *PIF8*, *PIF4*, *PIF5*, and *PIF7* visualized by hierarchical clustering (supports Figure 1).

Supplemental Figure 3. Increased expression of *PIL1* and *PIL2* mRNAs induced by PIF8 in far-red light (supports Figure 3).

Supplemental Figure 4. Hypocotyl lengths of *pif8 phyA* and *pif8 phyB* double mutants in far-red light (supports Figure 3).

Supplemental Figure 5. PIF8 does not promote hypocotyl elongation in the shade (supports Figure 3).

Supplemental Figure 6. Light-independent expression of transgenic *PIF8* mRNA in the *PIF8-OX cop1* mutant (supports Figure 6).

Supplemental Figure 7. Preferential interaction between PIF5 and phyA in vitro (supports Figure 2).

Supplemental Figure 8. Inhibition of blue light responses by PIF8 (supports Figure 3).

Supplemental Table 1. List of primers used in this study.

Supplemental Table 2. ANOVA tables.

Supplemental File 1. Sequence alignment for phylogenetic analysis of Arabidopsis, tomato, and rice PIFs and PILs (supports Figure 1).

Supplemental File 2. Tree file for phylogenetic analysis of Arabidopsis, tomato, and rice PIFs and PILs (supports Figure 1).

ACKNOWLEDGMENTS

This work was supported by the National Research Foundation of Korea (2018R1A3B1052617).

AUTHOR CONTRIBUTIONS

J.O., E.P., and G.C. designed the experiments; J.O., E.P., K.S., and G.B. performed the experiments; J.O. and G.C. wrote the article.

Received July 11, 2019; revised October 25, 2019; accepted November 14, 2019; published November 15, 2019.

REFERENCES

Al-Sady, B., Ni, W., Kircher, S., Schäfer, E., and Quail, P.H. (2006). Photoactivated phytochrome induces rapid PIF3 phosphorylation prior to proteasome-mediated degradation. Mol. Cell **23:** 439–446.

Bae, G., and Choi, G. (2008). Decoding of light signals by plant phytochromes and their interacting proteins. Annu. Rev. Plant Biol. **59:** 281–311.

Balcerowicz, M., Fittinghoff, K., Wirthmueller, L., Maier, A., Fackendahl, P., Fiene, G., Koncz, C., and Hoecker, U. (2011). Light exposure of Arabidopsis seedlings causes rapid de-stabilization as well as selective post-translational inactivation of the repressor of photomorphogenesis SPA2. Plant J. **65:** 712–723.

Bauer, D., Viczián, A., Kircher, S., Nobis, T., Nitschke, R., Kunkel, T., Panigrahi, K.C., Adám, E., Fejes, E., Schäfer, E., and Nagy, F. (2004). Constitutive photomorphogenesis 1 and multiple photoreceptors control degradation of phytochrome interacting factor 3, a transcription factor required for light signaling in Arabidopsis. Plant Cell **16:** 1433–1445.

Bu, Q., Zhu, L., Dennis, M.D., Yu, L., Lu, S.X., Person, M.D., Tobin, E.M., Browning, K.S., and Huq, E. (2011). Phosphorylation by CK2 enhances the rapid light-induced degradation of phytochrome interacting factor 1 in Arabidopsis. J. Biol. Chem. **286:** 12066–12074.

Casal, J.J., Yanovsky, M.J., and Luppi, J.P. (2000). Two photobiological pathways of phytochrome A activity, only one of which shows dominant negative suppression by phytochrome B. Photochem. Photobiol. **71:** 481–486.

Castillon, A., Shen, H., and Huq, E. (2009). Blue light induces degradation of the negative regulator phytochrome interacting factor 1 to promote photomorphogenic development of Arabidopsis seedlings. Genetics **182:** 161–171.

Chen, S., Lory, N., Stauber, J., and Hoecker, U. (2015). Photoreceptor specificity in the light-induced and COP1-mediated rapid degradation of the repressor of photomorphogenesis SPA2 in Arabidopsis. PLoS Genet. **11:** e1005516.

Clack, T., Mathews, S., and Sharrock, R.A. (1994). The phytochrome apoprotein family in Arabidopsis is encoded by five genes: The sequences and expression of PHYD and PHYE. Plant Mol. Biol. **25:** 413–427.

Clough, S.J., and Bent, A.F. (1998). Floral dip: A simplified method for Agrobacterium-mediated transformation of *Arabidopsis thaliana*. Plant J. **16:** 735–743.

Cordeiro, A.M., Figueiredo, D.D., Tepperman, J., Borba, A.R., Lourenço, T., Abreu, I.A., Ouwerkerk, P.B., Quail, P.H., Margarida Oliveira, M., and Saibo, N.J. (2016). Rice phytochrome-interacting factor protein OsPIF14 represses OsDREB1B gene expression through an extended N-box and interacts preferentially with the active form of phytochrome B. Biochim. Biophys. Acta **1859:** 393–404.

de Lucas, M., Davière, J.M., Rodríguez-Falcón, M., Pontin, M., Iglesias-Pedraz, J.M., Lorrain, S., Fankhauser, C., Blázquez, M.A., Titarenko, E., and Prat, S. (2008). A molecular framework for light and gibberellin control of cell elongation. Nature **451:** 480–484.

Dong, J., Ni, W., Yu, R., Deng, X.W., Chen, H., and Wei, N. (2017). Light-dependent degradation of PIF3 by SCF(EBF1/2) promotes a photomorphogenic response in Arabidopsis. Curr. Biol. **27:** 2420–2430.e2426.

Duek, P.D., Elmer, M.V., van Oosten, V.R., and Fankhauser, C. (2004). The degradation of HFR1, a putative bHLH class transcription factor involved in light signaling, is regulated by phosphorylation and requires COP1. Curr. Biol. **14:** 2296–2301.

Feng, S., et al. (2008). Coordinated regulation of *Arabidopsis thaliana* development by light and gibberellins. Nature **451:** 475–479.

Franklin, K.A. (2008). Shade avoidance. New Phytol. **179:** 930–944.

Franklin, K.A., and Quail, P.H. (2010). Phytochrome functions in Arabidopsis development. J. Exp. Bot. **61:** 11–24.

Fujimori, T., Yamashino, T., Kato, T., and Mizuno, T. (2004). Circadian-controlled basic/helix-loop-helix factor, PIL6, implicated in light-signal transduction in *Arabidopsis thaliana*. Plant Cell Physiol. **45:** 1078–1086.

Galvão, V.C., and Fankhauser, C. (2015). Sensing the light environment in plants: Photoreceptors and early signaling steps. Curr. Opin. Neurobiol. **34:** 46–53.

Gambetta, G.A., and Lagarias, J.C. (2001). Genetic engineering of phytochrome biosynthesis in bacteria. Proc. Natl. Acad. Sci. USA **98:** 10566–10571.

Gao, Y., Ren, X., Qian, J., Li, Q., Tao, H., and Chen, J. (2019). The phytochrome-interacting family of transcription factors in maize (*Zea mays* L.): Identification, evolution, and expression analysis. Acta Physiol. Plant. **41:** 8.

Gendrel, A.-V., Lippman, Z., Yordan, C., Colot, V., and Martienssen, R.A. (2002). Dependence of heterochromatic histone H3 methylation patterns on the Arabidopsis gene DDM1. Science **297:** 1871–1873.

Goodstein, D.M., Shu, S., Howson, R., Neupane, R., Hayes, R.D., Fazo, J., Mitros, T., Dirks, W., Hellsten, U., Putnam, N., and Rokhsar, D.S. (2012). Phytozome: A comparative platform for green plant genomics. Nucleic Acids Res. **40:** D1178–D1186.

Gu, D., Chen, C.Y., Zhao, M., Zhao, L., Duan, X., Duan, J., Wu, K., and Liu, X. (2017). Identification of HDA15-PIF1 as a key repression module directing the transcriptional network of seed germination in the dark. Nucleic Acids Res. **45:** 7137–7150.

He, Y., Li, Y., Cui, L., Xie, L., Zheng, C., Zhou, G., Zhou, J., and Xie, X. (2016). Phytochrome B negatively affects cold tolerance by regulating *OsDREB1* gene expression through phytochrome interacting factor-like protein OsPIL16 in rice. Front. Plant Sci. **7:** 1963.

Hoecker, U. (2017). The activities of the E3 ubiquitin ligase COP1/SPA, a key repressor in light signaling. Curr. Opin. Plant Biol. **37:** 63–69.

Hoecker, U., and Quail, P.H. (2001). The phytochrome A-specific signaling intermediate SPA1 interacts directly with COP1, a constitutive repressor of light signaling in Arabidopsis. J. Biol. Chem. **276:** 38173–38178.

Hornitschek, P., Kohnen, M.V., Lorrain, S., Rougemont, J., Ljung, K., López-Vidriero, I., Franco-Zorrilla, J.M., Solano, R., Trevisan, M., Pradervand, S., Xenarios, I., and Fankhauser, C. (2012). Phytochrome interacting factors 4 and 5 control seedling growth in changing light conditions by directly controlling auxin signaling. Plant J. **71:** 699–711.

Hornitschek, P., Lorrain, S., Zoete, V., Michielin, O., and Fankhauser, C. (2009). Inhibition of the shade avoidance response by formation of non-DNA binding bHLH heterodimers. EMBO J. **28:** 3893–3902.

Huang, X., Ouyang, X., and Deng, X.W. (2014). Beyond repression of photomorphogenesis: Role switching of COP/DET/FUS in light signaling. Curr. Opin. Plant Biol. **21:** 96–103.

Huq, E., Al-Sady, B., Hudson, M., Kim, C., Apel, K., and Quail, P.H. (2004). PHYTOCHROME-INTERACTING FACTOR 1 is a critical bHLH regulator of chlorophyll biosynthesis. Science **305:** 1937–1941.

Huq, E., and Quail, P.H. (2002). PIF4, a phytochrome-interacting bHLH factor, functions as a negative regulator of phytochrome B signaling in Arabidopsis. EMBO J. **21:** 2441–2450.

Inoue, K., Nishihama, R., Kataoka, H., Hosaka, M., Manabe, R., Nomoto, M., Tada, Y., Ishizaki, K., and Kohchi, T. (2016). Phytochrome signaling is mediated by PHYTOCHROME INTERACTING FACTOR in the liverwort *Marchantia polymorpha*. Plant Cell **28:** 1406–1421.

Jang, I.C., Yang, J.Y., Seo, H.S., and Chua, N.H. (2005). HFR1 is targeted by COP1 E3 ligase for post-translational proteolysis during phytochrome A signaling. Genes Dev. **19:** 593–602.

Jeong, J., and Choi, G. (2013). Phytochrome-interacting factors have both shared and distinct biological roles. Mol. Cells **35:** 371–380.

Ji, X., Du, Y., Li, F., Sun, H., Zhang, J., Li, J., Peng, T., Xin, Z., and Zhao, Q. (2019). The basic helix-loop-helix transcription factor, OsPIL15, regulates grain size via directly targeting a purine permease gene OsPUP7 in rice. Plant Biotechnol. J. **17:** 1527–1537.

Jung, J.H., et al. (2016). Phytochromes function as thermosensors in Arabidopsis. Science **354:** 886–889.

Khanna, R., Huq, E., Kikis, E.A., Al-Sady, B., Lanzatella, C., and Quail, P.H. (2004). A novel molecular recognition motif necessary for targeting photoactivated phytochrome signaling to specific basic helix-loop-helix transcription factors. Plant Cell **16:** 3033–3044.

Khanna, R., Shen, Y., Marion, C.M., Tsuchisaka, A., Theologis, A., Schäfer, E., and Quail, P.H. (2007). The basic helix-loop-helix transcription factor PIF5 acts on ethylene biosynthesis and phytochrome signaling by distinct mechanisms. Plant Cell **19:** 3915–3929.

Kidokoro, S., Maruyama, K., Nakashima, K., Imura, Y., Narusaka, Y., Shinwari, Z.K., Osakabe, Y., Fujita, Y., Mizoi, J., Shinozaki, K., and Yamaguchi-Shinozaki, K. (2009). The phytochrome-interacting factor PIF7 negatively regulates DREB1 expression under circadian control in Arabidopsis. Plant Physiol. **151:** 2046–2057.

Kim, D.H., Yamaguchi, S., Lim, S., Oh, E., Park, J., Hanada, A., Kamiya, Y., and Choi, G. (2008). SOMNUS, a CCCH-type zinc finger protein in Arabidopsis, negatively regulates light-dependent seed germination downstream of PIL5. Plant Cell **20:** 1260–1277.

Kim, H., Kim, S.T., Ryu, J., Choi, M.K., Kweon, J., Kang, B.C., Ahn, H.M., Bae, S., Kim, J., Kim, J.S., and Kim, S.G. (2016a). A simple, flexible and high-throughput cloning system for plant genome editing via CRISPR-Cas system. J. Integr. Plant Biol. **58:** 705–712.

Kim, J., Kang, H., Park, J., Kim, W., Yoo, J., Lee, N., Kim, J., Yoon, T.Y., and Choi, G. (2016b). PIF1-interacting transcription factors and their binding sequence elements determine the in vivo targeting sites of PIF1. Plant Cell **28:** 1388–1405.

Kim, J., Song, K., Park, E., Kim, K., Bae, G., and Choi, G. (2016c). Epidermal phytochrome B inhibits hypocotyl negative gravitropism non-cell-autonomously. Plant Cell **28:** 2770–2785.

Kim, J., Yi, H., Choi, G., Shin, B., Song, P.S., and Choi, G. (2003). Functional characterization of phytochrome interacting factor 3 in phytochrome-mediated light signal transduction. Plant Cell **15:** 2399–2407.

Kim, K., Shin, J., Lee, S.H., Kweon, H.S., Maloof, J.N., and Choi, G. (2011). Phytochromes inhibit hypocotyl negative gravitropism by regulating the development of endodermal amyloplasts through phytochrome-interacting factors. Proc. Natl. Acad. Sci. USA **108:** 1729–1734.

Klepikova, A.V., Kasianov, A.S., Gerasimov, E.S., Logacheva, M.D., and Penin, A.A. (2016). A high resolution map of the *Arabidopsis thaliana* developmental transcriptome based on RNA-seq profiling. Plant J. **88:** 1058–1070.

Klose, C., Viczián, A., Kircher, S., Schäfer, E., and Nagy, F. (2015). Molecular mechanisms for mediating light-dependent nucleo/cytoplasmic partitioning of phytochrome photoreceptors. New Phytol. **206:** 965–971.

Kriventseva, E.V., Kuznetsov, D., Tegenfeldt, F., Manni, M., Dias, R., Simão, F.A., and Zdobnov, E.M. (2019). OrthoDB v10: Sampling the diversity of animal, plant, fungal, protist, bacterial and viral genomes for evolutionary and functional annotations of orthologs. Nucleic Acids Res. **47:** D807–D811.

Kumar, I., Swaminathan, K., Hudson, K., and Hudson, M.E. (2016). Evolutionary divergence of phytochrome protein function in *Zea mays* PIF3 signaling. J. Exp. Bot. **67:** 4231–4240.

Kumar, S., Stecher, G., Li, M., Knyaz, C., and Tamura, K. (2018). MEGA X: Molecular evolutionary genetics analysis across computing platforms. Mol. Biol. Evol. **35:** 1547–1549.

Kunihiro, A., Yamashino, T., and Mizuno, T. (2010). PHYTOCHROME-INTERACTING FACTORS PIF4 and PIF5 are implicated in the regulation of hypocotyl elongation in response to blue light in *Arabidopsis thaliana*. Biosci. Biotechnol. Biochem. **74:** 2538–2541.

Labun, K., Montague, T.G., Gagnon, J.A., Thyme, S.B., and Valen, E. (2016). CHOPCHOP v2: A web tool for the next generation of CRISPR genome engineering. Nucleic Acids Res. **44:** W272–W276.

Lee, N., and Choi, G. (2017). Phytochrome-interacting factor from Arabidopsis to liverwort. Curr. Opin. Plant Biol. **35:** 54–60.

Lee, N., Park, J., Kim, K., and Choi, G. (2015). The transcriptional coregulator LEUNIG_HOMOLOG inhibits light-dependent seed germination in Arabidopsis. Plant Cell **27:** 2301–2313.

Legris, M., Klose, C., Burgie, E.S., Rojas, C.C., Neme, M., Hiltbrunner, A., Wigge, P.A., Schäfer, E., Vierstra, R.D., and Casal, J.J. (2016). Phytochrome B integrates light and temperature signals in Arabidopsis. Science **354:** 897–900.

Leivar, P., and Monte, E. (2014). PIFs: Systems integrators in plant development. Plant Cell **26:** 56–78.

Leivar, P., Monte, E., Al-Sady, B., Carle, C., Storer, A., Alonso, J.M., Ecker, J.R., and Quail, P.H. (2008a). The Arabidopsis phytochrome-interacting factor PIF7, together with PIF3 and PIF4, regulates responses to prolonged red light by modulating phyB levels. Plant Cell **20:** 337–352.

Leivar, P., Monte, E., Oka, Y., Liu, T., Carle, C., Castillon, A., Huq, E., and Quail, P.H. (2008b). Multiple phytochrome-interacting bHLH transcription factors repress premature seedling photomorphogenesis in darkness. Curr. Biol. **18:** 1815–1823.

Leivar, P., and Quail, P.H. (2011). PIFs: Pivotal components in a cellular signaling hub. Trends Plant Sci. **16:** 19–28.

Li, F.W., and Mathews, S. (2016). Evolutionary aspects of plant photoreceptors. J. Plant Res. **129:** 115–122.

Li, F.W., Melkonian, M., Rothfels, C.J., Villarreal, J.C., Stevenson, D.W., Graham, S.W., Wong, G.K., Pryer, K.M., and Mathews, S. (2015). Phytochrome diversity in green plants and the origin of canonical plant phytochromes. Nat. Commun. **6:** 7852.

Li, L., et al. (2012). Linking photoreceptor excitation to changes in plant architecture. Genes Dev. **26:** 785–790.

Li, L., Zhang, Q., Pedmale, U.V., Nito, K., Fu, W., Lin, L., Hazen, S.P., and Chory, J. (2014). PIL1 participates in a negative feedback

loop that regulates its own gene expression in response to shade. Mol. Plant **7:** 1582–1585.

Lian, H.L., He, S.B., Zhang, Y.C., Zhu, D.M., Zhang, J.Y., Jia, K.P., Sun, S.X., Li, L., and Yang, H.Q. (2011). Blue-light-dependent interaction of cryptochrome 1 with SPA1 defines a dynamic signaling mechanism. Genes Dev. **25:** 1023–1028.

Ling, J.J., Li, J., Zhu, D., and Deng, X.W. (2017). Noncanonical role of *Arabidopsis* COP1/SPA complex in repressing BIN2-mediated PIF3 phosphorylation and degradation in darkness. Proc. Natl. Acad. Sci. USA **114:** 3539–3544.

Liu, B., Zuo, Z., Liu, H., Liu, X., and Lin, C. (2011). Arabidopsis cryptochrome 1 interacts with SPA1 to suppress COP1 activity in response to blue light. Genes Dev. **25:** 1029–1034.

Liu, X., Chen, C.Y., Wang, K.C., Luo, M., Tai, R., Yuan, L., Zhao, M., Yang, S., Tian, G., Cui, Y., Hsieh, H.L., and Wu, K. (2013). PHYTOCHROME INTERACTING FACTOR3 associates with the histone deacetylase HDA15 in repression of chlorophyll biosynthesis and photosynthesis in etiolated Arabidopsis seedlings. Plant Cell **25:** 1258–1273.

Llorente, B., D'Andrea, L., Ruiz-Sola, M.A., Botterweg, E., Pulido, P., Andilla, J., Loza-Alvarez, P., and Rodriguez-Concepcion, M. (2016). Tomato fruit carotenoid biosynthesis is adjusted to actual ripening progression by a light-dependent mechanism. Plant J. **85:** 107–119.

Lorrain, S., Allen, T., Duek, P.D., Whitelam, G.C., and Fankhauser, C. (2008). Phytochrome-mediated inhibition of shade avoidance involves degradation of growth-promoting bHLH transcription factors. Plant J. **53:** 312–323.

Lorrain, S., Trevisan, M., Pradervand, S., and Fankhauser, C. (2009). Phytochrome interacting factors 4 and 5 redundantly limit seedling de-etiolation in continuous far-red light. Plant J. **60:** 449–461.

Lu, X.D., Zhou, C.M., Xu, P.B., Luo, Q., Lian, H.L., and Yang, H.Q. (2015). Red-light-dependent interaction of phyB with SPA1 promotes COP1-SPA1 dissociation and photomorphogenic development in Arabidopsis. Mol. Plant **8:** 467–478.

Luo, Q., Lian, H.L., He, S.B., Li, L., Jia, K.P., and Yang, H.Q. (2014). COP1 and phyB physically interact with PIL1 to regulate its stability and photomorphogenic development in Arabidopsis. Plant Cell **26:** 2441–2456.

Ma, D., Li, X., Guo, Y., Chu, J., Fang, S., Yan, C., Noel, J.P., and Liu, H. (2016). Cryptochrome 1 interacts with PIF4 to regulate high temperature-mediated hypocotyl elongation in response to blue light. Proc. Natl. Acad. Sci. USA **113:** 224–229.

Majee, M., et al. (2018). KELCH F-BOX protein positively influences Arabidopsis seed germination by targeting PHYTOCHROME-INTERACTING FACTOR1. Proc. Natl. Acad. Sci. USA **115:** E4120–E4129.

Martínez-García, J.F., Huq, E., and Quail, P.H. (2000). Direct targeting of light signals to a promoter element-bound transcription factor. Science **288:** 859–863.

Nagatani, A. (2004). Light-regulated nuclear localization of phytochromes. Curr. Opin. Plant Biol. **7:** 708–711.

Nakamura, Y., Kato, T., Yamashino, T., Murakami, M., and Mizuno, T. (2007). Characterization of a set of phytochrome-interacting factor-like bHLH proteins in *Oryza sativa*. Biosci. Biotechnol. Biochem. **71:** 1183–1191.

Ni, W., Xu, S.L., Chalkley, R.J., Pham, T.N., Guan, S., Maltby, D.A., Burlingame, A.L., Wang, Z.Y., and Quail, P.H. (2013). Multisite light-induced phosphorylation of the transcription factor PIF3 is necessary for both its rapid degradation and concomitant negative feedback modulation of photoreceptor phyB levels in Arabidopsis. Plant Cell **25:** 2679–2698.

Ni, W., Xu, S.L., González-Grandío, E., Chalkley, R.J., Huhmer, A.F.R., Burlingame, A.L., Wang, Z.Y., and Quail, P.H. (2017). PPKs mediate direct signal transfer from phytochrome photoreceptors to transcription factor PIF3. Nat. Commun. **8:** 15236.

Ni, W., Xu, S.L., Tepperman, J.M., Stanley, D.J., Maltby, D.A., Gross, J.D., Burlingame, A.L., Wang, Z.Y., and Quail, P.H. (2014). A mutually assured destruction mechanism attenuates light signaling in Arabidopsis. Science **344:** 1160–1164.

Nozue, K., Covington, M.F., Duek, P.D., Lorrain, S., Fankhauser, C., Harmer, S.L., and Maloof, J.N. (2007). Rhythmic growth explained by coincidence between internal and external cues. Nature **448:** 358–361.

Oh, E., Kang, H., Yamaguchi, S., Park, J., Lee, D., Kamiya, Y., and Choi, G. (2009). Genome-wide analysis of genes targeted by PHYTOCHROME INTERACTING FACTOR 3-LIKE5 during seed germination in Arabidopsis. Plant Cell **21:** 403–419.

Oh, E., Kim, J., Park, E., Kim, J.I., Kang, C., and Choi, G. (2004). PIL5, a phytochrome-interacting basic helix-loop-helix protein, is a key negative regulator of seed germination in *Arabidopsis thaliana*. Plant Cell **16:** 3045–3058.

Oh, E., Yamaguchi, S., Hu, J., Yusuke, J., Jung, B., Paik, I., Lee, H.S., Sun, T.P., Kamiya, Y., and Choi, G. (2007). PIL5, a phytochrome-interacting bHLH protein, regulates gibberellin responsiveness by binding directly to the GAI and RGA promoters in Arabidopsis seeds. Plant Cell **19:** 1192–1208.

Oh, E., Yamaguchi, S., Kamiya, Y., Bae, G., Chung, W.I., and Choi, G. (2006). Light activates the degradation of PIL5 protein to promote seed germination through gibberellin in Arabidopsis. Plant J. **47:** 124–139.

Osterlund, M.T., and Deng, X.W. (1998). Multiple photoreceptors mediate the light-induced reduction of GUS-COP1 from Arabidopsis hypocotyl nuclei. Plant J. **16:** 201–208.

Osterlund, M.T., Hardtke, C.S., Wei, N., and Deng, X.W. (2000). Targeted destabilization of HY5 during light-regulated development of Arabidopsis. Nature **405:** 462–466.

Pacín, M., Legris, M., and Casal, J.J. (2013). COP1 re-accumulates in the nucleus under shade. Plant J. **75:** 631–641.

Pacín, M., Legris, M., and Casal, J.J. (2014). Rapid decline in nuclear constitutive photomorphogenesis1 abundance anticipates the stabilization of its target elongated hypocotyl5 in the light. Plant Physiol. **164:** 1134–1138.

Park, E., Kim, J., Lee, Y., Shin, J., Oh, E., Chung, W.-I., Liu, J.R., and Choi, G. (2004). Degradation of phytochrome interacting factor 3 in phytochrome-mediated light signaling. Plant Cell Physiol. **45:** 968–975.

Park, E., Kim, Y., and Choi, G. (2018). Phytochrome B requires PIF degradation and sequestration to induce light responses across a wide range of light conditions. Plant Cell **30:** 1277–1292.

Park, E., Park, J., Kim, J., Nagatani, A., Lagarias, J.C., and Choi, G. (2012). Phytochrome B inhibits binding of phytochrome-interacting factors to their target promoters. Plant J. **72:** 537–546.

Park, J., Bae, S., and Kim, J.S. (2015). Cas-Designer: A web-based tool for choice of CRISPR-Cas9 target sites. Bioinformatics **31:** 4014–4016.

Pfeiffer, A., Shi, H., Tepperman, J.M., Zhang, Y., and Quail, P.H. (2014). Combinatorial complexity in a transcriptionally centered signaling hub in Arabidopsis. Mol. Plant **7:** 1598–1618.

Pham, V.N., Kathare, P.K., and Huq, E. (2018a). Dynamic regulation of PIF5 by COP1-SPA complex to optimize photomorphogenesis in Arabidopsis. Plant J. **96:** 260–273.

Pham, V.N., Kathare, P.K., and Huq, E. (2018b). Phytochromes and phytochrome interacting factors. Plant Physiol. **176:** 1025–1038.

Pham, V.N., Xu, X., and Huq, E. (2018c). Molecular bases for the constitutive photomorphogenic phenotypes in *Arabidopsis*. Development **145:** dev169870.

Possart, A., Xu, T., Paik, I., Hanke, S., Keim, S., Hermann, H.M., Wolf, L., Hiß, M., Becker, C., Huq, E., Rensing, S.A., and Hiltbrunner, A. (2017). Characterization of phytochrome interacting factors from the moss *Physcomitrella patens* illustrates conservation of phytochrome signaling modules in land plants. Plant Cell **29:** 310–330.

Qiu, Y., Li, M., Kim, R.J., Moore, C.M., and Chen, M. (2019). Daytime temperature is sensed by phytochrome B in Arabidopsis through a transcriptional activator HEMERA. Nat. Commun. **10:** 140.

Qiu, Y., Li, M., Pasoreck, E.K., Long, L., Shi, Y., Galvão, R.M., Chou, C.L., Wang, H., Sun, A.Y., Zhang, Y.C., Jiang, A., and Chen, M. (2015). HEMERA couples the proteolysis and transcriptional activity of PHYTOCHROME INTERACTING FACTORs in Arabidopsis photomorphogenesis. Plant Cell **27:** 1409–1427.

Rockwell, N.C., Su, Y.S., and Lagarias, J.C. (2006). Phytochrome structure and signaling mechanisms. Annu. Rev. Plant Biol. **57:** 837–858.

Roig-Villanova, I., and Martínez-García, J.F. (2016). Plant responses to vegetation proximity: A whole life avoiding shade. Front. Plant Sci. **7:** 236.

Rosado, D., Gramegna, G., Cruz, A., Lira, B.S., Freschi, L., de Setta, N., and Rossi, M. (2016). Phytochrome Interacting Factors (PIFs) in *Solanum lycopersicum*: Diversity, evolutionary history and expression profiling during different developmental processes. PLoS One **11:** e0165929.

Saeed, A.I., et al. (2003). TM4: A free, open-source system for microarray data management and analysis. Biotechniques **34:** 374–378.

Sakuraba, Y., Kim, E.Y., Han, S.H., Piao, W., An, G., Todaka, D., Yamaguchi-Shinozaki, K., and Paek, N.C. (2017). Rice Phytochrome-Interacting Factor-Like1 (OsPIL1) is involved in the promotion of chlorophyll biosynthesis through feed-forward regulatory loops. J Exp Bot **68 (15):** 4103–4114.

Sheerin, D.J., Menon, C., zur Oven-Krockhaus, S., Enderle, B., Zhu, L., Johnen, P., Schleifenbaum, F., Stierhof, Y.D., Huq, E., and Hiltbrunner, A. (2015). Light-activated phytochrome A and B interact with members of the SPA family to promote photomorphogenesis in Arabidopsis by reorganizing the COP1/SPA complex. Plant Cell **27:** 189–201.

Shen, H., Moon, J., and Huq, E. (2005). PIF1 is regulated by light-mediated degradation through the ubiquitin-26S proteasome pathway to optimize photomorphogenesis of seedlings in Arabidopsis. Plant J. **44:** 1023–1035.

Shen, H., Zhu, L., Castillon, A., Majee, M., Downie, B., and Huq, E. (2008). Light-induced phosphorylation and degradation of the negative regulator PHYTOCHROME-INTERACTING FACTOR1 from Arabidopsis depend upon its direct physical interactions with photoactivated phytochromes. Plant Cell **20:** 1586–1602.

Shen, Y., Khanna, R., Carle, C.M., and Quail, P.H. (2007). Phytochrome induces rapid PIF5 phosphorylation and degradation in response to red-light activation. Plant Physiol. **145:** 1043–1051.

Shi, H., Zhong, S., Mo, X., Liu, N., Nezames, C.D., and Deng, X.W. (2013). HFR1 sequesters PIF1 to govern the transcriptional network underlying light-initiated seed germination in Arabidopsis. Plant Cell **25:** 3770–3784.

Shin, A.Y., Han, Y.J., Baek, A., Ahn, T., Kim, S.Y., Nguyen, T.S., Son, M., Lee, K.W., Shen, Y., Song, P.S., and Kim, J.I. (2016). Evidence that phytochrome functions as a protein kinase in plant light signalling. Nat. Commun. **7:** 11545.

Shin, J., Kim, K., Kang, H., Zulfugarov, I.S., Bae, G., Lee, C.H., Lee, D., and Choi, G. (2009). Phytochromes promote seedling light responses by inhibiting four negatively-acting phytochrome-interacting factors. Proc. Natl. Acad. Sci. USA **106:** 7660–7665.

Soy, J., Leivar, P., González-Schain, N., Martín, G., Diaz, C., Sentandreu, M., Al-Sady, B., Quail, P.H., and Monte, E. (2016). Molecular convergence of clock and photosensory pathways through PIF3-TOC1 interaction and co-occupancy of target promoters. Proc. Natl. Acad. Sci. USA **113:** 4870–4875.

Todaka, D., et al. (2012). Rice phytochrome-interacting factor-like protein OsPIL1 functions as a key regulator of internode elongation and induces a morphological response to drought stress. Proc. Natl. Acad. Sci. USA **109:** 15947–15952.

von Arnim, A.G., and Deng, X.-W. (1994). Light inactivation of Arabidopsis photomorphogenic repressor COP1 involves a cell-specific regulation of its nucleocytoplasmic partitioning. Cell **79:** 1035–1045.

Wagner, D., Koloszvari, M., and Quail, P.H. (1996). Two small spatially distinct regions of phytochrome B are required for efficient signaling rates. Plant Cell **8:** 859–871.

Wang, C.C., Meng, L.H., Gao, Y., Grierson, D., and Fu, D.Q. (2018). Manipulation of light signal transduction factors as a means of modifying steroidal glycoalkaloids accumulation in tomato leaves. Front. Plant Sci. **9:** 437.

Xie, C., Zhang, G., An, L., Chen, X., and Fang, R. (2019). Phytochrome-interacting factor-like protein OsPIL15 integrates light and gravitropism to regulate tiller angle in rice. Planta **250:** 105–114.

Xu, T., and Hiltbrunner, A. (2017). PHYTOCHROME INTERACTING FACTORs from *Physcomitrella patens* are active in Arabidopsis and complement the pif quadruple mutant. Plant Signal. Behav. **12:** e1388975.

Xu, X., Paik, I., Zhu, L., and Huq, E. (2015). Illuminating progress in phytochrome-ediated light signaling pathways. Trends Plant Sci. **20:** 641–650.

Yamashino, T., Matsushika, A., Fujimori, T., Sato, S., Kato, T., Tabata, S., and Mizuno, T. (2003). A link between circadian-controlled bHLH factors and the APRR1/TOC1 quintet in *Arabidopsis thaliana*. Plant Cell Physiol. **44:** 619–629.

Yang, J., Lin, R., Sullivan, J., Hoecker, U., Liu, B., Xu, L., Deng, X.W., and Wang, H. (2005). Light regulates COP1-mediated degradation of HFR1, a transcription factor essential for light signaling in Arabidopsis. Plant Cell **17:** 804–821.

Zhang, B., Holmlund, M., Lorrain, S., Norberg, M., Bakó, L., Fankhauser, C., and Nilsson, O. (2017). BLADE-ON-PETIOLE proteins act in an E3 ubiquitin ligase complex to regulate PHYTOCHROME INTERACTING FACTOR 4 abundance. eLife **6:** e26759.

Zhang, Y., Mayba, O., Pfeiffer, A., Shi, H., Tepperman, J.M., Speed, T.P., and Quail, P.H. (2013). A quartet of PIF bHLH factors provides a transcriptionally centered signaling hub that regulates seedling morphogenesis through differential expression-patterning of shared target genes in Arabidopsis. PLoS Genet. **9:** e1003244.

Zheng, X., et al. (2013). Arabidopsis phytochrome B promotes SPA1 nuclear accumulation to repress photomorphogenesis under far-red light. Plant Cell **25:** 115–133.

Zhou, J., Liu, Q., Zhang, F., Wang, Y., Zhang, S., Cheng, H., Yan, L., Li, L., Chen, F., and Xie, X. (2014a). Overexpression of OsPIL15, a phytochrome-interacting factor-like protein gene, represses etiolated seedling growth in rice. J. Integr. Plant Biol. **56:** 373–387.

Zhou, P., Song, M., Yang, Q., Su, L., Hou, P., Guo, L., Zheng, X., Xi, Y., Meng, F., Xiao, Y., Yang, L., and Yang, J. (2014b). Both PHYTOCHROME RAPIDLY REGULATED1 (PAR1) and PAR2 promote seedling photomorphogenesis in multiple light signaling pathways. Plant Physiol. **164:** 841–852.

Zhu, J.Y., Oh, E., Wang, T., and Wang, Z.Y. (2016). TOC1-PIF4 interaction mediates the circadian gating of thermoresponsive growth in Arabidopsis. Nat. Commun. **7:** 13692.

Zhu, L., Bu, Q., Xu, X., Paik, I., Huang, X., Hoecker, U., Deng, X.W., and Huq, E. (2015). CUL4 forms an E3 ligase with COP1 and SPA to promote light-induced degradation of PIF1. Nat. Commun. **6:** 7245.